

Anonymous Referee #1

The authors carefully revised the manuscript in response to the previous reviewer comments. Data issues and analysis approaches were well examined. Thus the results seem to be robust. However, I believe that this study is still not a substantial contribution to our understanding of global vegetation/Earth system dynamics. As the manuscript has a strong focus on the state of NDVI and land carbon exchange in the year 2015, it is a very particular description of the 2015 situation. This particular focus was already criticised during the previous stage of the review. The authors slightly expanded the focus in the revised version but decided to still keep the strong focus on the year 2015. Although I think that this focus does not make the manuscript very interesting for the scientific community, I can okay it. As the results are robust, I suggest to accept the manuscript as it is and to let the scientific community decide about the scientific significance of these results.

[Response] We appreciate the reviewer's efforts to review our manuscript and the general positive view on our revised manuscript. We have in fact used the year 2015 as an illustrative natural experiment to examine the responses of land ecosystems to a combination of extreme greening and the occurrence of a very strong El Niño event. We strived to make a balance between general analysis of land carbon dynamics and vegetation greenness and climate variations, by using all years when data are available, and a focus on the special case of 2015. Throughout the result and discussion sections, the interpretation of carbon dynamics of 2015 is the assumed focus but it is always put into a context of all historical years, since the "abnormal" character of this year can only be understood from comparison with other years. The focus on the year of 2015 as a special case to study carbon cycle responses to ENSO events does not make the current work less interesting to the scientific community. In fact, on the most recent 10th International Carbon Dioxide Conference in Switzerland, there was a full session dedicated to the 2015 ENSO event

(<https://www.conftool.com/icdc10/index.php?page=browseSessions&presentations=hide>), demonstrating the scientific community's interest on its influences on the earth system. Therefore, we contend that our study can come as a timely one and could be of interest to the community.

There are two key points in this manuscript that we hope can bring valuable insights to the scientific community. (1) It is almost taken granted that growing-season vegetation greenness in the northern hemisphere leads to land carbon sink, while our study highlights the importance of carbon dynamics at seasonal time scale. The decoupling of greening and land carbon uptake outside the growing season, and the enhanced autumn release due to warming or an intrinsic coupling of enhanced spring-summer uptake and autumn release, can actually offset the greening-induced carbon sink during the growing season. (2) We identified an extremely large transition to a carbon source (the largest over the data record of 1981–2015) in the tropics and southern hemisphere from the third to the fourth season, concomitant with the development of the strong El Niño in 2015. This finding highlights the potential future impact on land sink by the projected increase in the frequency of extreme El Niño events caused by the anthropogenic climate change.

In line with the suggestions made by the 2nd reviewer, we have revised the sections of abstract, introduction, discussion and conclusion in the updated version of the manuscript, to make clearer the scientific implications of our findings and to guide the

readers better interpret the results in the manuscript. The two points aforementioned are also described more clearly in the revised manuscript. All revised texts in the manuscript are tracked in blue.

Anonymous Referee #2

The authors have made very significant changes to the paper, and have addressed the reviewer comments in a relatively profound way. The article contains a very detailed and rich analysis, and I think that the balance between the year 2015 and other years is now adequate. The authors also improved the discussions of links to previous studies on the relations between the carbon cycle, vegetation greenness and climate anomalies. The scientific methods are very well documented and appear reasonable to me, and the results support the author's conclusions.

There is one aspect that I think the authors did not address so well, which is to work out a clear motivation for their study and a message that emerges from their results. As a meticulous case study for the year 2015, I think that the paper can be useful for other scientists in the same field. Having said that, the authors may reconsider if the visibility of their paper might be improved by some additional changes, especially in the abstract, introduction, and conclusions section.

To me, the fact that greening and carbon loss can occur together due to different seasons, locations and processes, invokes the question what the future trends of these changes are going to be. For example, would an increased ENSO frequency or amplitude have the potential to overcompensate the carbon uptake due to warming in the extratropics? Can the author's results be used for a simple back-of-the-envelope calculation (for example, an extrapolation of their results into the future) to estimate a range of possibilities? Which sources of uncertainty in particular should be reduced in order to get a better estimate? Can the increased respiration in autumn in mid-latitudes overcompensate the increased uptake in spring, or does this only reflect the larger annual cycle with increasing overall uptake?

I understand that these may be questions too general and complex to answer. But my point is that using such kinds of questions at least as an orientation to guide the reader through the manuscript can improve its readability by pointing out the benefits that readers would have from spending time on the article. The aspects above are implicitly (and sometimes explicitly) already mentioned in the manuscript, but they are hidden in a large haystack of details. The very long and detailed documentation of results still leaves me a bit confused about how to link these results to the big questions about the carbon cycle. I believe that the authors have the expertise to work out these links in a more explicit way, without the need for much extra analysis.

[Response] We thank the reviewer's effort to review our manuscript and for the general appreciation of our efforts to revise the manuscript. In this updated version of the manuscript, we focused on revising the sections of abstract, introduction, discussion and conclusion, according to the reviewer's suggestions to make clearer the motivations of our study, and to guide the readers in interpreting the findings. The reviewers have given a few questions as examples that are relevant with our research objectives. Our revisions of the introduction and abstract are centered on these and other similar

questions. Please refer to the updated manuscript. All revised texts in the manuscript are tracked in blue.

Minor comments:

- The overall language of the article is good, but I would recommend that a native speaker takes a final look. There are some issues with missing articles especially. examples:

[Response] All following suggested language corrections below are accepted. The language of the manuscript has been improved by professional copy-editing service.

line 482: outside the growing season,

line 486: a strong transition to a carbon source,

line 487: observations showing a strong dependence of...

line 558: The validity period of ... is 2004-2015, although data for the whole time span is available.

line 785: still not good English – should read “apparent paradox”

line 859: more common would be “linked to”, or “associated with”

line 969: tropical vegetation shows

line 1034: decoupled outside the growing season ... The transition into a carbon source

- lines 559-562: I actually like the explanation in the response to my previous review more than the version in the article because it really explains what the validity period is and why the estimates deteriorate outside. Readers who are less familiar with these technical details might not understand this paragraph as it is.

[Response] We replaced the relevant text with the explanations provided as the response to previous review comments and hope it is now more clear.

- line 683: The reason to remove year 1993 seems to be that it is an outlier and the authors conclude that the method fails in this case. But what assures the authors that a similar problem does not occur in other years as well, with a smaller effect on the results?

[Response] To some extent yes. The Jena inversion shows not such extreme transition as is seen in the CAMS inversion in 1993. In the case of strong negative transitions in the tropics between Q3 and Q4 in 2015, both CAMS and Jena show consistent transitions and the strong negative transitions are associated with a lower-than-normal annual land carbon sink in 2015. The year 1993, however, shows a reasonably strong annual carbon sink by the CAMS inversion and thus a negative carbon transition of -2.85 Pg C lower than -4σ is considered as an outlier.

- line 822: What is meant with a “first-order difference”? Couldn’t one just remove “first-order”?

[Response] We removed “first-order” here to remove the unnecessary complexity.

- line 1041: What is meant with opposing ENSO events?

[Response] We mean opposing ENSO phases (i.e., the cold phase of La Nina versus the warm phase of El Niño). This is now specified in the text.

- line 1044: I am still quite sceptical about the use of the term “abrupt” in this context. I

would prefer the term “large climate anomalies”. An abrupt shift usually implies consequences that are permanent.

[Response] We use “abrupt” here to mean more of “extreme” shift, such as the shift from an extremely low precipitation anomaly in Q3 to an extremely high one in Q4 for the region of temperate Northern Hemisphere (TeNH) as shown in Fig. S5g–h. We replaced “abrupt” by “extreme”.

- line 1073-1075: This statement goes into the direction that I am driving at above and should be explained a bit more. It almost reads like an afterthought, but could be a major argument for the purpose of this study in the introduction. Why is this study an interesting test bed, and how? And after having done the analysis, how should one proceed to evaluate the models and gain understanding? Hence, the authors may want to fill this interesting statement with some more flavour and serve it as an appetizer instead of a dessert.

[Response] We have revised the sections of abstract, introduction, discussion and conclusion and have use questions as such proposed by the reviewer to lay down a concrete background for our study and to guide the readers to interpret our findings. Please refer to the revisions made in these sections.

1 **Vegetation greenness and land carbon flux anomalies associated with climate**
2 **variations: a focus on the year 2015**

3
4 Chao Yue¹, Philippe Ciais¹, Ana Bastos¹, Frederic Chevallier¹, Yi Yin¹, Christian Rödenbeck²,
5 Taejin Park³

6
7 ¹Laboratoire des Sciences du Climat et de l'Environnement, CEA-CNRS-UVSQ, UMR8212,
8 91191 Gif-sur-Yvette, France

9 ²Max Planck Institute for Biogeochemistry, Jena, Germany.

10 ³Department of Earth and Environment, Boston University, Boston, MA 02215, USA

11
12 Corresponding author: Chao Yue, chao.yue@lscce.ipsl.fr

13
14 **Abstract**

15
16 Understanding the variations in global land carbon uptake, and their driving mechanisms, is
17 essential if we are to predict future carbon cycle feedbacks on global environmental changes.
18 Satellite observations of vegetation greenness have shown consistent greening across the globe
19 over the past three decades. Such greening has driven the increasing land carbon sink, especially
20 over the growing season in northern latitudes. On the other hand, interannual variations in land
21 carbon uptake are strongly influenced by El Niño–Southern Oscillation (ENSO) climate
22 variations. Marked reductions in land uptake and strong positive anomalies in the atmospheric
23 CO₂ growth rates occur during El Niño events. Here we use the year 2015 as a natural
24 experiment to examine the possible response of land ecosystems to a combination of vegetation
25 greening and an El Niño event. The year 2015 was the greenest year since 2000 according to
26 satellite observations, but a record atmospheric CO₂ growth rate also occurred due to a weaker
27 than usual land carbon sink. Two atmospheric inversions indicate that the year 2015 had a higher
28 than usual northern land carbon uptake in boreal spring and summer, consistent with the positive
29 greening anomaly and strong warming. This strong uptake was, however, followed by a larger
30 source of CO₂ in the autumn. For the year 2015, enhanced autumn carbon release clearly offset
31 the extra uptake associated with greening during the summer. This finding leads us to speculate

32 that a long-term greening trend may foster more uptakes during the growing season, but no large
33 increase in annual carbon sequestration. For the tropics and Southern Hemisphere, a strong
34 transition towards a large carbon source for the last three months of 2015 is discovered,
35 concomitant with El Niño development. This transition of terrestrial tropical CO₂ fluxes between
36 two consecutive seasons is the largest ever found in the inversion records. The strong transition
37 to a carbon source in the tropics with the peak of El Niño is consistent with historical
38 observations, but the detailed mechanisms underlying such extreme transition remain to be
39 elucidated.

40

41 **1 Introduction**

42

43 The first monitoring station for background atmospheric CO₂ concentration was established on
44 Mauna Loa in 1958. Its record shows that atmospheric CO₂ has continued to rise as
45 anthropogenic carbon emissions have increased. However, annual atmospheric CO₂ growth rates
46 (AGR) are lower than those implied by anthropogenic emissions alone, because land ecosystems
47 and the oceans have absorbed part of the emitted CO₂ (Canadell et al., 2007; Le Quéré et al.,
48 2016). At multi-decadal timescale, carbon uptake by land and ocean has kept pace with growing
49 carbon emissions (Ballantyne et al., 2012; Li et al., 2016), exerting a strong negative feedback to
50 global change. Over land, increasing carbon uptake is consistent with worldwide vegetation
51 greening as revealed by satellite observations (Zhu et al., 2016). Long-term warming and CO₂
52 fertilization have contributed to growing-season greening and increasing land carbon uptake in
53 northern latitudes, which further leads to a markedly increasing seasonal atmospheric CO₂
54 amplitude (Forkel et al., 2016; Graven et al., 2013; Myneni et al., 1997). At the same time, large
55 year-to-year fluctuations occur in the terrestrial carbon sink especially over tropical lands. These
56 fluctuations mainly occur in response to climate variations induced by El Niño–Southern
57 Oscillation (ENSO) (Wang et al., 2013, 2014) and other occasional events such as volcanic
58 eruptions (Gu et al., 2003). The occurrence of El Niño events often leads to elevated
59 temperatures with reductions in precipitation over tropical lands; these cause sustained droughts
60 that substantially reduce the land carbon uptake (Doughty et al., 2015). These ENSO-associated
61 tropical land uptake variations have translated into large variations in atmospheric CO₂ growth
62 rates, which are found to be significantly correlated with tropical land temperature anomalies

63 (Wang et al., 2014).

64

65 Understanding such driving mechanisms and variations in land carbon uptake is essential if we
66 are to predict future carbon cycle feedbacks on global environmental changes — including
67 climate change. Growing-season normalized difference vegetation index (NDVI) observed by
68 the moderate-resolution imaging spectroradiometer (MODIS) aboard the Terra satellite has
69 consistently increased since 2000 over northern latitudes (Bastos et al., 2017). The positive link
70 between seasonal NDVI and vegetation photosynthesis is well established for deciduous forests
71 in temperate and boreal biomes (Gamon et al., 1995), and NDVI is often assumed as a surrogate
72 for vegetation growth. Nevertheless, it is unclear whether, on an annual timescale, higher NDVI
73 anomalies are indeed always associated with higher carbon uptake anomalies. A few studies have
74 reported important seasonal coupling in vegetation greenness and land carbon uptake in mid to
75 high latitudes, with summer drought likely compensating for enhanced spring uptake (Angert et
76 al., 2005; Wolf et al., 2016). While spring warming may enhance vegetation growth and carbon
77 uptake, autumn warming can lead to net carbon loss by enhancing respiration carbon loss (Piao
78 et al., 2008). Furthermore, greening and browning may occur in different regions within the same
79 growing season (Bastos et al., 2017), so that the associated consequence on land carbon
80 dynamics needs to be investigated. Such investigation on the relationship between seasonal
81 NDVI dynamics and land carbon uptake will help to predict future land carbon sink capacity.

82

83 El Niño events are often linked to enhanced drought conditions in Amazonian forest with
84 widespread increases in tree mortality and drops in ecosystem carbon storage (Phillips et al.,
85 2009). Fire emissions from Asian tropical regions also show nonlinear increase with drought
86 during El Niño, another factor that reduces land carbon sequestration (Field et al., 2016; Yin et
87 al., 2016). With future anthropogenic climate change, it is projected that the frequency of
88 extreme El Niño events will be doubled (Cai et al., 2014). It is not clear how future carbon
89 dynamics will respond to such a doubling of extreme El Niño events, or whether any extreme
90 phenomena in the carbon cycle might occur as a consequence. The year of 2015 is a good test
91 case for investigating El Niño-related phenomena because it contained the strongest El Niño
92 event since the one in 1997/98 and occurred at a time when unprecedented mean annual land
93 temperature was observed.

94
95 We use the year 2015 as a natural experiment to investigate the response of land ecosystems to a
96 combination of extreme greening and an El Niño event. The year 2015 had the greenest growing
97 season in the Northern Hemisphere since 2000, in particular over eastern North America and
98 large parts of Siberia (Bastos et al., 2017), and this was accompanied by the highest mean annual
99 global land temperature on record since 1880 ([https://www.ncdc.noaa.gov/cag/time-](https://www.ncdc.noaa.gov/cag/time-series/global/globe/land/yt/12/1880-2015)
100 [series/global/globe/land/yt/12/1880-2015](https://www.ncdc.noaa.gov/cag/time-series/global/globe/land/yt/12/1880-2015)). At the same time, a strong El Niño event developed
101 starting in the latter half of 2015. Elevated fire emissions in tropical Asia were reported (Huijnen
102 et al., 2016; Yin et al., 2016) and a severe drought was detected over eastern Amazonia
103 (Jiménez-Muñoz et al., 2016). As a result, in 2015 the global monthly atmospheric CO₂
104 concentration surpassed 400 μmol·mol⁻¹ (ppm) for the first time, with an unprecedented large
105 annual growth rate of 2.96±0.09 ppm yr⁻¹
106 (https://www.esrl.noaa.gov/gmd/ccgg/trends/global.html#global_growth). We examined global
107 and regional land-atmosphere carbon fluxes estimated from two atmospheric inversions over
108 1981-2015. Seasonal patterns in the land carbon uptake in 2015 relative to the long-term trend of
109 1981-2015 were examined and linked to extreme climate anomalies. To put the 2015 land
110 response into a historical context, we also examined the relationship between historical land
111 carbon uptake anomalies, and NDVI and climate anomalies, in order to infer general patterns in
112 factors driving the land carbon uptake anomalies. Our findings are expected to provide insights
113 into future land carbon cycle feedbacks to vegetation greening and climate variations.

114

115 **2 Data and methods**

116 **2.1 Data sets**

117 **2.1.1 Atmospheric inversion data**

118 We used two gridded land and ocean carbon uptake data sets based on atmospheric CO₂
119 observations, namely those from the Copernicus Atmosphere Monitoring Service (CAMS)
120 inversion system developed at LSCE (Chevallier et al., 2005, 2010) and the Jena CarboScope
121 inversion system developed at the MPI for Biogeochemistry, Jena (update of Rödenbeck, 2005;
122 Rödenbeck et al., 2003). Atmospheric inversions estimate land- and ocean-atmosphere net
123 carbon fluxes by minimizing a Bayesian cost function, accounting for the mismatch between the
124 observed and simulated atmospheric CO₂ mixing ratios. To do this, they use atmospheric CO₂

125 concentrations at measurement sites, combined with an atmospheric transport model and prior
126 information on fossil fuel carbon emissions and carbon exchange between the atmosphere and
127 land (and ocean). Detailed information on these two atmospheric inversions can be found in the
128 references above.

129

130 The CAMS inversion data (version r15v3) were provided for 1979–2015 with a weekly time-step
131 and a spatial resolution of 1.875° latitude and 3.75° longitude. The Jena CarboScope inversion
132 provides daily fluxes at a spatial resolution of 3.75° latitude and 5° longitude and offers a series
133 of runs. All runs provide data covering the whole period of 1979–2015, but they have different
134 validity periods that focus on using different sets of CO₂ measurement stations. Within the
135 validity period all employed stations have valid CO₂ observations, i.e., they have coherent and
136 complete measurements over time. The idea of validity period is to avoid spurious flux variations
137 resulting from a changing station network. It is optimal to examine temporal trend within the
138 validity period, but this does not mean the data outside this period are invalid and should be
139 discarded. From the Jena inversion runs, we selected s04_v3.8 (shortened as Jena04 in the main
140 text and the Supplementary Material). Jena04 used the largest number of measurement sites for
141 2015 and therefore had the most detailed constraint on carbon exchanges for this year (see
142 <http://www.bgc-jena.mpg.de/CarboScope/> for more details on other configurations). The validity
143 period of the Jena04 data is 2004–2015, but here we used the data available for the whole time
144 span of 1981–2015. This is necessary to provide both the large number of sites in 2015 and the
145 long historical period, which is needed to produce a robust anomaly estimate. We compared the
146 linear trends obtained over large latitudinal regions between the Jena04 run and the long
147 s81_v3.8 run (the latter has a validity period of 1981–2015 but far fewer sites are included than
148 in Jena04), and confirmed that the derived trends are similar. The same issue of evolving site
149 number and data coverage with time also occurs for the CAMS inversion, but the CAMS
150 inversion uses sites with at least a 5-year run of data. CAMS therefore has a denser (during the
151 recent decade) but temporally evolving data coverage than CarboScope.

152

153 Estimates of land and ocean net carbon uptakes for 1981–2015 from the Global Carbon Project
154 (GCP) (Le Quéré et al., 2016) were compared with the inversion data. For this purpose, an
155 annual global carbon flux of 0.45 Pg C yr⁻¹ is subtracted from the inversion-derived land carbon

Chao Yue 6/9/y 10:24

Supprimé: The evolving network in CAMS causes changes in inverted CO₂ fluxes that are superimposed on changes from biogeochemical drivers during the whole period.

161 uptakes and is added to ocean carbon uptakes to account for the pre-industrial land-to-ocean
162 carbon fluxes induced by river transport (Jacobson et al., 2007), following Le Quéré et al. (2016).
163 Ocean carbon uptakes in the GCP estimates are based on the mean CO₂ sink estimated for the
164 1990s from observations, and the trend and variability in the ocean CO₂ sink for 1959–2015 from
165 global ocean biogeochemistry models. Estimates of land carbon uptake in the GCP estimates are
166 calculated as the difference between anthropogenic emissions, atmospheric CO₂ growth and the
167 ocean sink. In summary, the estimates of land and ocean carbon uptake in the GCP estimates are
168 largely independent from the two inversions used here, except that the CO₂ records from
169 atmospheric stations that are used in the inversions are also used in the GCP estimates.

170

171 **2.1.2 Atmospheric CO₂ growth rates, NDVI and climate data**

172 Atmospheric CO₂ growth rates were retrieved from the Global Monitoring Division, Earth
173 System Research Laboratory (ESRL), NOAA
174 (<http://www.esrl.noaa.gov/gmd/ccgg/trends/global.html>). We used NDVI data between 2000 and
175 2015 from MODIS Terra Collection 6 (Didan, 2015), at a resolution of 0.05° and a 16-day time-
176 step. NDVI data are processed from MODIS land surface reflectance data and thoroughly
177 corrected for atmospheric effects. We were strict in applying quality assurance (QA) controls to
178 maintain a distinct seasonal trajectory of vegetative radiometric observations and minimize
179 spurious signals (e.g., snow or cloud). Detected unexpected non-vegetative observations were
180 first excluded and then filled using the adaptive Savitzky–Golay filter (Chen et al., 2004; Jönsson
181 and Eklundh, 2004). The Savitzky–Golay filter is a simplified convolution over a set of
182 consecutive values with weighting coefficients given by a polynomial least-squares-fit within the
183 filter window (Savitzky and Golay, 1964). After this procedure, the linearly interpolated daily
184 NDVI data were used to calculate mean seasonal NDVI and re-gridded at 0.5° resolution, with
185 pixels of seasonal NDVI lower than 0.1 being further masked to ensure robustness. We examined
186 four seasons: Q1 (January–March), Q2 (April–June), Q3 (July–September) and Q4 (October–
187 December). Climate fields are from the ERA interim reanalysis (Dee et al., 2011) at 0.5°
188 resolution and monthly time-step. We used air temperature, precipitation and volumetric soil
189 water content (%) integrated over the soil column to a depth of 2.89 m.

190

191 **2.1.3 Indices for El Niño–Southern Oscillation states and fire emission data**

192 We examined the seasonal variations of the carbon cycle in 2015 in relation to ENSO events and
193 compared the 2015 El Niño event with that of 1997–1998. The Multivariate ENSO Index (MEI,
194 <http://www.esrl.noaa.gov/psd/enso/mei/>, Wolter and Timlin, 2011) was used to indicate the
195 ENSO state. MEI is a composite index calculated as the first un-rotated principal component of
196 six ENSO-relevant variables (including sea level pressure and sea-surface temperature) over the
197 tropical Pacific for each of twelve sliding two-monthly seasons. MEI has been widely used in
198 previous studies of land carbon dynamics as an indicator of ENSO states (Nemani et al., 2003;
199 van der Werf et al., 2008). The twelve two-monthly MEI values for each year are summed to
200 obtain the annual MEI. The interannual variations in climate and land carbon uptake are linked
201 with MEI to infer a general relationship between land carbon dynamics and ENSO climate
202 oscillations. To examine the potential role of fire emissions in the land carbon balance in 2015,
203 we used the GFED4s carbon emission data at daily time-step and 0.25° spatial resolution
204 (<http://www.globalfiredata.org/data.html>). Monthly fire-carbon emissions were calculated for the
205 regions and were examined for 1997–2015.

206

207 **2.2 Data analysis**

208 **2.2.1 NDVI rank analysis and greening trend**

209 We first examine the vegetation greenness status in the year 2015. Given a season and a pixel,
210 the annual time series of seasonal NDVI for 2000–2015 were ranked in ascending order so that
211 each year could be labelled by a rank, with 1 being the lowest and 16 being the highest. A spatial
212 map of NDVI rank was then obtained for each year for the given season (Fig. S1). A composite
213 map was made for 2015, by merging pixels with the highest rank of all four seasons in 2015 (Fig.
214 1a). Vegetated area fraction with the highest rank for different years was obtained, with the sum
215 of these fractions yielding unity. This procedure was repeated for all four seasons to generate
216 four seasonal time series, with each time series containing the vegetation land fractions with
217 highest NDVI for different years (Fig. 1b). Note that NDVI values for the Northern Hemisphere
218 for Q1 and Q4 mostly fall outside the growing season (although October is frequently considered
219 within the growing season and some evergreen coniferous forests show significant
220 photosynthetic activities in March in regions with mild winters, e.g., Tanja et al., 2003), so that a
221 valid NDVI might not necessarily be associated with significant seasonal vegetation activity.
222 However, we expect that this issue will be partly alleviated by our applied rigorous QA control

223 in preprocessing and a minimum threshold of 0.1 on seasonal NDVI. Such seasonal segregation
224 is adopted mainly because of its general applicability across the globe, especially for tropical
225 ecosystems where seasonality in vegetation activities is minimal.

226

227 **2.2.2 Analysis of land carbon uptake dynamics associated with climate variations**

228 Annual land and ocean carbon uptake and carbon emissions from the two inversions were
229 calculated for the globe over their period of overlap, 1981–2015. AGRs from NOAA/ESRL over
230 1981–2015 were converted into Pg C using a conversion factor of 2.12 Pg C ppm⁻¹ (Ballantyne
231 et al., 2012; Prather et al., 2012; Quéré et al., 2016), in order to examine the closure of the global
232 carbon balance in the inversion data. The conversion factor used here assumes that the entire
233 atmosphere is well mixed over one year. We attributed the record high AGR in 2015 into
234 individual components of emissions and sinks. The record high AGR in 2015 was a composite
235 effect collectively determined by carbon emissions from fossil fuel burning and industry, and
236 land and ocean carbon uptakes. All these were impacted by an historical trend (Fig. 2).

237 Therefore, to understand the factors contributing to 2015's record AGR, we separated it into a
238 long-term trend and interannual anomalies. Annual time series of carbon emissions, land and
239 ocean carbon uptakes, and AGRs from NOAA/ESRL over 1981–2015 were linearly de-trended.
240 The percentages of anomalies in carbon emissions, land and ocean sink in 2015 to the 2015 AGR
241 anomaly were then calculated as relative contributions by each factor to the 2015 AGR anomaly.

242

243 Seasonal land carbon uptake anomaly time series were also calculated by subtracting the same
244 linear trend for 1981–2015. The globe was divided into three latitude bands: boreal Northern
245 Hemisphere (BoNH, latitude > 45°N), temperate Northern Hemisphere (TeNH, 23.5° < latitude
246 < 45°N), and tropics and extratropical Southern Hemisphere (TroSH, latitude < 23.5°N). The
247 BoNH and TeNH are grouped as Boreal and temperate Northern Hemisphere (BoTeNH, latitude >
248 23.5°N) when examining seasonal carbon transitions. Seasonal land carbon uptake anomalies
249 were then calculated for each region and the whole globe, with positive anomalies indicating
250 enhanced sink (or reduced source) against the linear trend (i.e., the normal state), and negative
251 ones indicating the opposite. The same seasonal linear de-trending was also performed for
252 climate fields of air temperature, precipitation and soil water content. The relationship between
253 anomalies in land carbon uptake, and temperature and precipitation are examined using partial

Chao Yue 4/9/13 13:55

Supprimé: Therefore, we must put 2015's record high AGR into an historical perspective. For example, if 2015 shows a large increase in carbon emissions accompanied by droughts (browning) in the Northern Hemisphere and the tropics, then the highest AGR should not come as a great surprise.

262 correlation coefficients in a multivariate linear regression framework with an ordinary least
263 squares method. The relationships between seasonal land uptake anomalies and NDVI anomalies
264 were also examined using simple linear regression.

265

266 We then examined especially the seasonal anomalies of land carbon uptake in 2015 and the
267 carbon uptake transitions between two consecutive seasons, to reveal any extreme phenomena in
268 the land carbon cycle that might lead to the abnormally high AGR in 2015. Seasonal land carbon
269 uptake transitions are calculated as the land sink anomaly in a given season minus that of the
270 previous one. When examining transitions of land carbon uptake anomalies by the CAMS
271 inversion, we found the year 1993 had an extreme negative Q3→Q4 global transition (-2.85 Pg
272 C within 6 months, $< -4\sigma$, the second lowest being the year 2015 with -1.0 Pg C) albeit with a
273 reasonable annual land carbon uptake (3.75 Pg C yr⁻¹). This is linked to an extreme high Q3 and
274 low Q4 uptake in this year, which could not be explained by any known carbon cycle
275 mechanisms. This is thus identified as a result of numerical instability of the inversion system for
276 that release and consequently the year 1993 has been removed from all the aforementioned
277 seasonal analyses. [However, we identified that the temporal trends for annual and seasonal land
278 carbon uptakes show almost no change whether or not including the year 1993.](#)

279

280 **3 Results**

281 **3.1 Vegetation greening in 2015**

282 Figure 1a illustrates where and when higher-than-normal greening conditions were observed in
283 different seasons of the year 2015, compared to other years of 2000–2015 (see Supplementary
284 Material Fig. S1 for the greenness distribution of each season). On average over the four seasons
285 of 2015, 16% of vegetated land shows record seasonal NDVI. The year with the second highest
286 NDVI is 2014 with 9% vegetated area having record NDVI. An increase of the record-breaking
287 NDVI occurrence over time is clearly seen in Fig. 1b. In short, 2015 clearly stands out as a
288 greening outlier, having the highest proportion of vegetated land being the greenest for all four
289 seasons except for the first season (despite the fact that for Q1, 2015 is still the third highest, Q1
290 = January to March).

291

292 For boreal and temperate regions of the Northern Hemisphere, the seasons with highest NDVI in

293 2015 are dominated by Q2 and Q3 (Q2 = April to June; Q3 = July to September), corresponding
294 to the growing season from spring to early autumn (Supplementary Material Fig. S2). A
295 pronounced greening anomaly in Q2 occurred in western to central Siberia, western Canada and
296 Alaska, and eastern and southern Asia (Supplementary Material Fig. S1). Central and eastern
297 Siberia and eastern North America showed marked greening in Q3. Strong and widespread
298 greening also occurred in the tropics during Q3 across Amazonia and the savanna (or cerrado) of
299 eastern South America and tropical Africa, but this strong positive greening signal greatly
300 diminished in Q4 (Q4 = October to December) especially in central to eastern Amazonia with the
301 development of El Niño (Supplementary Material Fig. S1). Overall, the strongest greening in
302 2015 across the globe is dominated by northern lands (latitude > 23.5°N), while for the northern
303 tropics (0–23.5°N) only moderately strong greening is found, and for the Southern Hemisphere
304 the greening of 2015 is close to the average state for the period of 2000–2015 (Supplementary
305 Material Fig. S3). The extreme growing-season greening in the northern land is confirmed as
306 being a robust result by Bastos et al. (2017), who used Terra MODIS NDVI data with different
307 quality control procedures, and consistency is also confirmed between Terra and Aqua sensors
308 (Fig. S1 in Bastos et al., 2017).

309

310 **3.2 Global carbon balance for 1981-2015**

311 Figure 2 shows the time series of fossil fuel burning and industry carbon emissions,
312 NOAA/ESRL AGR rates linked to ENSO climate oscillations as indicated by the Multivariate
313 ENSO Index (MEI), and land and ocean carbon sinks for the common period of the two
314 inversions (1981–2015) and the estimates by the Global Carbon Project (GCP). Emissions show
315 a clear increase with time, however AGRs are more variable. The record high AGR of 2.96 ppm
316 in 2015 exceeds those in all previous years including the extreme El Niño event in 1997–98,
317 despite much higher annual emissions in 2015. Interannual variability in AGR is mainly caused
318 by fluctuations in the land carbon sink, with Pearson’s correlation coefficients between de-
319 trended AGR and land sink < -0.8 ($p < 0.01$) for both inversions (Pearson’s correlation coefficient
320 between de-trended AGR and MEI being 0.27, $p < 0.1$). The root mean square differences
321 between inversion and GCP carbon sinks are 0.70 and 0.65 Pg C yr⁻¹ for CAMS and Jena04
322 respectively for the land, and ~0.5 Pg C yr⁻¹ for the ocean for both inversions, within the
323 uncertainties of 0.8 and 0.5 Pg C yr⁻¹ over 1981–2015, respectively for land and ocean as

324 reported by GCP. The interannual variability of de-trended sink anomalies for the land agrees
325 well between the inversions and the GCP estimates (with Pearson's correlation coefficient being
326 0.9 for both inversions, $p < 0.01$).

327

328 For 2015, the prescribed anthropogenic carbon emissions in the CAMS inversion are 9.9 Pg C yr^{-1}
329 ¹, of which 2.0 Pg C are absorbed by ocean, 1.7 Pg C by land ecosystems, with 6.2 Pg C
330 remaining in the atmosphere, which matches the AGR from background stations of 6.3 Pg C
331 assuming a conversion factor of $2.12 \text{ Pg C ppm}^{-1}$ (Ballantyne et al., 2012; Le Quéré et al., 2016)
332 and considering a measurement uncertainty in AGR of 0.09 ppm (0.2 Pg C) for 2015. When land
333 carbon fluxes from the inversion are linearly de-trended over 1981-2015, the terrestrial sink in
334 2015 is 1.2 Pg C lower than normal (i.e., the trend value), but this is not an extreme value — it is
335 only the seventh weakest sink since 1981. This weaker land uptake accounts for 82% of the
336 positive AGR anomaly, which is 1.45 Pg C in 2015 by subtracting a linear temporal trend.
337 Jena04 yields an AGR in 2015 that is 0.13 ppm lower than the AGR based on background
338 stations only, a difference close to the observation uncertainty. After removing the linear trends
339 over time similarly as for the CAMS inversion, the land carbon uptake anomaly for Jena04 is -
340 0.3 Pg C yr^{-1} in 2015, or 20% of the observed AGR anomaly, the remaining being explained by a
341 positive anomaly in fossil fuel emissions (34%), a negative anomaly in the ocean sink (20%),
342 and the difference between modelled AGR and NOAA/ESRL reported AGR. Note that the land
343 sink given by the GCP data for 2015 is much lower than in the two inversions, with de-trended
344 anomaly lower than that of CAMS, indicating an even larger contribution from land to the high
345 anomaly of AGR.

346

347 In general, the warm phases of ENSO events are associated with positive anomalies in land air
348 temperature, negative precipitation anomalies, and lower land carbon uptake anomalies (Fig. 3),
349 this is consistent with previous studies (Cox et al., 2013; Wang et al., 2014). The lower
350 precipitation during El Niño is due to a shift of precipitation from tropical land to the ocean
351 (Adler et al., 2003), and higher land temperature might be due to reduced evaporative cooling.
352 The two extreme El Niño years of 1997 and 2015 have rather close MEI values. Compared with
353 the 'standard' El Niño state of temperature and precipitation represented by the regression line,
354 the year 1997 was relatively 'cool' and 'wet', while 2015 was rather 'warm' and 'dry' (with an

355 extremely negative precipitation anomaly). Year 1998 has a smaller value of MEI than
356 1997/2015, but has a higher temperature anomaly than 2015, and a much lower land carbon
357 uptake anomaly than 1997 and 2015 in both inversions, while the land carbon uptake anomalies
358 in 1997 and 2015 are similar. More detailed comparison of these three years and their carbon
359 cycle dynamics will be presented in the discussion section.

360

361 **3.3 Seasonal land carbon uptake dynamics associated with climate variations with a focus** 362 **on 2015**

363

364 Figure 4 shows the partial correlation coefficients between anomalies in seasonal land carbon
365 uptake and those in seasonal temperature and precipitation for different regions. The simple,
366 individual (univariate) linear relationships between de-trended anomalies in land carbon fluxes
367 and those in temperature and precipitation, are presented in the Supplementary Material (Fig. S4
368 and S5). Land carbon fluxes show consistent relationships with temperature between the two
369 inversions for BoNH: a positive relationship for Q2 and a negative one for the other three
370 seasons (with Q1 by Jena04 being the only one with a non-significant correlation). Partial
371 correlations between land fluxes and precipitation are absent or non-significant for BoNH. This
372 points to the fact that vegetation productivity in BoNH is in principle dominated by temperature,
373 with warmer spring and early summer (Q2, April–June) enhancing vegetation net carbon uptake,
374 but a higher temperature in later summer, autumn and early winter reducing the land capacity to
375 sequester carbon, consistent with previous studies (Piao et al., 2008). For TeNH, a significant
376 negative relationship is found between land fluxes by the CAMS inversion and temperature for
377 Q3, and both inversions show negative relationships between land fluxes and precipitation for
378 Q4, probably due to enhanced early autumn respiration under wetter conditions. For TroSH, land
379 carbon uptakes in Q1, Q2 and Q4 are all negatively related with temperature ($p < 0.05$ for both
380 inversions), while increase in precipitation in Q1 is found to be associated with enhanced land
381 uptake.

382

383 To explain the apparent paradox in 2015 between the strong greening and an only moderate
384 terrestrial uptake, we examined in detail the seasonal land carbon flux anomalies in 2015 (Fig. 5,
385 refer to Supplementary Material Fig. S6 for the spatial distribution of flux anomalies). At

386 seasonal scale, both inversions indicate positive carbon uptake anomalies during Q2 and Q3 for
387 boreal and temperate Northern Hemisphere (BoTeNH, latitude $> 23.5^{\circ}\text{N}$), consistent with
388 marked greening in central to eastern Siberia, eastern Europe and Canada (Fig. 1) as outlined
389 above. Indeed, both BoNH and TeNH show positive relationships between seasonal land carbon
390 flux anomalies and NDVI anomalies for Q2 and Q3, with BoNH showing moderate greenness
391 (after a linear trend is removed) for Q3, and TeNH showing extreme greenness for Q2 in 2015
392 (Supplementary Material Fig. S7). However, an extreme follow-up negative (source) anomaly
393 occurred in Q4 (Fig. 5a). These negative anomalies were lower than the 10th percentile of all
394 anomalies in Q4 over time for both inversions and they partly cancelled the extra uptake in Q2
395 and Q3. As a result, on an annual timescale, the CAMS inversion shows an almost neutral land
396 flux anomaly in BoTeNH, while the Jena04 inversion still indicates a significant positive annual
397 anomaly.

398

399 For the tropics and extratropical Southern Hemisphere (TroSH, latitude $< 23.5^{\circ}\text{N}$), both
400 inversions show a weak negative land carbon anomaly for Q1 (mean value of -0.10 Pg C) in
401 2015, moderate anomalies in Q2 (of differing signs, with a negative one of -0.3 Pg C in CAMS
402 and a positive one of 0.2 Pg C in Jena04). Q3 anomalies are almost carbon neutral for both
403 inversions. In stark contrast, between Q3 and Q4, both inversions show a strong shift towards an
404 abnormally big land carbon source (i.e., negative anomalies of ~ -0.7 Pg C against a carbon
405 source expected from the linear trend, lower than 10th percentile over time in both inversions).
406 On an annual timescale, CAMS shows a large negative anomaly of -1.2 Pg C. For Jena04, sink
407 and source effects in Q1–Q3 cancelled each other, leaving the annual anomaly the same as in Q4.

408

409 Over the globe, the Jena04 inversion shows an abnormally strong sink during Q2 (normal state
410 being a net carbon sink), owing to synergy of enhanced Q2 uptakes in both BoTeNH and TroSH.
411 This abnormally enhanced uptake partly counteracted the strong shift towards a source in Q4
412 (normal state being a net carbon source), leaving a small negative annual land carbon balance of
413 -0.3 Pg C. For the CAMS inversion, because of the co-occurrence of enhanced carbon release in
414 BoTeNH and the sudden shift towards a large carbon source in TroSH both in Q4 (normal state
415 for both being a net carbon source), the land shows a strong global shift towards being a source
416 in Q4, leaving a negative annual carbon anomaly of -1.2 Pg C (i.e., carbon sink being reduced

417 compared with the normal state).

418

419 These consistent results from both inversions point to very strong seasonal shifts in the land
420 carbon balance as an emerging feature of 2015. We thus calculated *transitions* in land carbon
421 uptake anomaly as the difference in flux anomalies between two consecutive seasons (defined as
422 the anomaly in a given season minus that in the previous one) for all years of the period 1982-
423 2015 (Fig. 6). The ranks of transitions for different seasons relative to other years between the
424 two inversions are broadly similar, except for Q1→Q2 and Q2→Q3 in TroSH, mainly due to the
425 differences between the two inversions in seasonal land-carbon uptake anomaly in Q2 (Fig. 5b).
426 On the global scale, both inversions show an extreme transition to a negative uptake anomaly for
427 Q3→Q4, with 2015 being the largest transition of the period 1982-2015 (a transition towards an
428 enhanced carbon source of -1.0 Pg C in six months). The abnormal transitions for Q3→Q4 on
429 the global scale are located in the TroSH region, where both inversions show that during 1982-
430 2015 the largest transition occurred in 2015. For BoTeNH, both inversions showed strong
431 transitions towards positive anomaly for Q1→Q2; however, the same strong transition towards
432 source anomaly occurred in Q3→Q4, partly cancelling the sink effects during growing seasons.

433

434 **4 Discussion**

435 **4.1 Land carbon uptake dynamics with climate variations in northern latitudes and** 436 **seasonal transitions of land carbon uptake in 2015**

437 The two inversions consistently allocate a strong positive carbon uptake anomaly in the region of
438 BoTeNH during spring, which persists through the summer (Q2–Q3): an extreme sink anomaly
439 is estimated in Q2 by Jena04, but a more moderate one by CAMS (still above the 75th
440 percentile). The strong sinks in Q2 in both inversions are dominated by temperate Northern
441 Hemisphere regions (TeNH, 23.5° < latitude < 45°N, Supplementary Material Fig. S8). For this
442 region, both inversions show strong positive correlation between carbon uptake anomalies and
443 NDVI in Q2, with an extremely high NDVI anomaly in 2015 (Supplementary Material Fig. S7f).
444 Thus, the strong sinks in Q2 are evidently linked to the extreme greening, while temperature and
445 precipitation anomalies were only moderate (Fig. S4f, Fig. S5f).

446

447 For Q3, an extreme carbon sink anomaly occurs in boreal Northern Hemisphere (BoNH, latitude >

448 45°N) in CAMS; however, an equally strong negative anomaly (i.e., reduced sink) was found in
449 TeNH in the same season, leaving the whole boreal and temperate Northern Hemisphere
450 (BoTeNH) only a moderately positive sink anomaly (Fig. S8). For TeNH alone, CAMS indicates
451 extreme seasonal shift from a positive anomaly in Q2 to a negative one in Q3. This implies
452 strong seasonal transitions resulting from enhanced ecosystem CO₂ release after growing-season
453 uptake [and the presence of seasonal coupling in land carbon dynamics](#). For TeNH in 2015,
454 NDVI persisted from a high extreme in Q2 to close to normal in Q3 (Fig. S7f, Fig. S7g), and
455 temperature remained moderate for both Q2 and Q3 (Fig. S4f, S4g), but precipitation shifted
456 from a moderate anomaly in Q2 to an extremely low one (Fig. S5f, S5g). In summary, the shift
457 from a high Q2 sink anomaly to a big Q3 source anomaly by CAMS might be linked to the shift
458 in precipitation and drought in Q3, such as the prevailing drought in Europe as shown in Fig. S9
459 (see also a detailed discussion of the European drought by Orth et al., 2016).

460

461 Jena04 inversion agrees with a higher-than-normal sink in TeNH ($23.5^\circ < \text{latitude} < 45^\circ\text{N}$)
462 during spring (Q2). It also reports a moderate positive anomaly for Q3 in BoNH, but does not
463 show a strong negative anomaly (i.e., reduced sink) in TeNH in Q3 as CAMS does (Fig. S8).
464 This is possibly related to differences in the measurement station data used, to different land
465 prior fluxes (from the ORCHIDEE model in CAMS, and the LPJ model in Jena CarboScope), or
466 to the fact that the Jena04 inversion has a larger a-priori spatial error correlation length for its
467 land fluxes (1275 km) than CAMS (500 km) (Chevallier et al., 2010; Rödenbeck et al., 2003).
468 Nonetheless, both inversions consistently indicate that the enhancement of CO₂ uptake during
469 spring and summer at the northern hemispheric scale was subsequently offset by an extreme
470 source anomaly in autumn (Q4).

471

472 The large carbon source anomalies in Q4 shown by the two inversions in BoTeNH seem to be
473 dominated by different factors in BoNH versus TeNH. In BoNH the source anomaly in 2015 is
474 more linked to elevated temperature in Q4, which shows a significant negative correlation with
475 carbon uptake anomalies by both inversions (Fig. S4d). In contrast, precipitation in Q4 has no
476 correlation with carbon uptake anomalies, and precipitation in 2015 was close to the normal state
477 (Fig. S5d). The prevailing high temperature in Q4 of 2015 is especially evident over most
478 northern America, and central to eastern Siberia and Europe (Supplementary Fig. S9a).

479

480 In TeNH, the roles of temperature and precipitation are reversed compared to BoNH. Q4
481 precipitation is found to have a significant negative correlation with land carbon uptake
482 anomalies for both inversions, and Q4 in 2015 was characterized by a very high precipitation
483 anomaly, leading to a reduced land carbon uptake (Fig. S5h). While temperature in Q4 of 2015
484 was moderately high, no significant correlation is found between carbon uptake anomalies and
485 temperature (Fig. S4h). However, for both BoNH and TeNH, NDVI remained moderately high
486 in Q4 of 2015 (Fig. S7d, S7h).

487

488 The positive relationship between land carbon uptake and temperature in Q2 (spring and early
489 summer), and a negative one for Q3 and Q4 (autumn) for BoNH, are in line with previous
490 studies. Several studies reported an enhanced greening during spring and summer in the Northern
491 Hemisphere (Myneni et al., 1997; Zhou et al., 2001), as driven by increasing spring and summer
492 temperatures (Barichivich et al., 2013; Nemani et al., 2003), leading to enhanced land carbon
493 uptake and a long-term increase in the seasonal amplitude of atmospheric CO₂ in northern
494 latitudes (Forkel et al., 2016; Graven et al., 2013). However, for autumn, even though ending of
495 growing season has been delayed because of autumn warming (Barichivich et al., 2013), land
496 carbon uptake termination time is found to have advanced as well, due to enhanced autumn
497 respiration (Piao et al., 2008), which ultimately reduced the annual net ecosystem carbon uptake
498 (Hadden and Grelle, 2016; Ueyama et al., 2014). For TeNH, we also found a significant negative
499 relationship between land carbon uptake anomalies and temperature for Q3 using the CAMS
500 inversion data, consistent with the enhanced respiration by autumn warming found in the
501 aforementioned studies. For Q4, however, both inversions point to decreasing land carbon
502 uptakes with increasing precipitation. This finding might be due to enhanced respiration resulting
503 from higher soil moisture content, but further site-scale examination is needed to confirm this
504 hypothesis.

505

506 For BoNH and TeNH, land carbon uptake anomalies are closely coupled with NDVI anomalies
507 for Q2 (positive correlation, albeit an insignificant one for TeNH Q2 using Jena04 data), but they
508 are generally de-coupled for Q3 and Q4, except that for Q3 of BoNH the CAMS-based land
509 carbon uptake shows positive correlation with NDVI. This suggests high NDVI in autumn might

510 not necessarily relate to a high land carbon uptake. There are two reasons. First, NDVI is found
511 to correlate well with leaf-level CO₂ uptake for deciduous forest for different seasons, but is
512 largely independent of leaf photosynthesis for evergreen forests (Gamon et al., 1995). Second,
513 even though a higher NDVI is associated with larger photosynthetic capacity and a higher gross
514 photosynthesis, autumn warming might increase ecosystem respiration more than photosynthesis,
515 leaving a net carbon source effect. Furthermore, other studies have also pointed out that severe
516 summer drought can negate the enhanced carbon uptake during warm springs (Angert et al.,
517 2005; Wolf et al., 2016).

518

519 **4.2 Seasonal land carbon uptake transitions in the tropics and influences of El Niño and** 520 **vegetation fire**

521

522 The strong transition to abnormal source in the tropics and extratropical Southern Hemisphere
523 was paralleled by a marked decrease in precipitation and an increase in temperature in Q4, with
524 the development of El Niño in Q2–Q3 (Supplementary Material Fig. S4I, S5I, S10). Here El
525 Niño development is indicated by the rise of the MEI and Oceanic Niño Index (ONI,
526 http://www.cpc.ncep.noaa.gov/products/analysis_monitoring/ensostuff/ONI_change.shtml). This
527 strong transition is consistent with the expected response of tropical and sub-tropical southern
528 ecosystems during previous El Niño events (Ahlström et al., 2015; Cox et al., 2013; Poulter et
529 al., 2014; Wang et al., 2013, 2014). The small abnormal source in Q1 in TroSH is consistent with
530 a low precipitation anomaly. While temperature anomalies are abnormally high in Q2 and Q3,
531 accompanied by extremely negative precipitation anomalies, the extremely low carbon flux in
532 Q4 is largely explained by temperature, because correlations between land carbon uptake and
533 precipitation in Q4 are very weak (Fig. S4i–l, Fig. S5i–l). Vegetation greenness has significant
534 positive correlation with land carbon uptake anomalies only for Q1 in the tropics, and for the rest
535 of the three seasons the correlation is very weak (Fig. S7i–l).

536

537 Compared with the 1997–98 El Niño, which had a slightly larger MEI value, the 2015 El Niño
538 started much earlier, with positive MEI and ONI appearing during the first half of 2014. Since
539 then and until Q3 and Q4 in 2015 when El Niño began to reach its peak, the tropics and Southern
540 Hemisphere saw continuous higher-than-normal temperatures, with continually decreasing

541 precipitation and accumulating deficit in soil water content (Supplementary Material Fig. S10).
542 From Q3 to Q4, a steep decline is further observed in both precipitation and soil moisture with
543 stagnating high temperature anomaly, which is probably a major cause of the strong shift
544 towards a carbon source anomaly. The CAMS inversion shows a carbon source anomaly in Q4
545 of 2015 slightly smaller than that in Q3 of 1997, while the Jena04 inversion shows almost equal
546 magnitudes of loss in land sink strength between these two extreme El Niño events. On the one
547 hand, El Niño in late 2015 started early and built upon the cumulative effects of the drought
548 since the beginning of the year; it thus came with larger negative anomaly in precipitation and
549 soil water content than the 1997–98 El Niño. This sequence of events might favour a stronger
550 land carbon source. On the other hand, the fire emission anomaly in the tropics in 2015 was less
551 than half of that in 1997 at the peak of El Niño (Fig. S10); this might have contributed to a
552 smaller land source anomaly in 2015 than in 1997–98.

553

554 El Niño events are usually associated with increased vegetation fires, which have a large impact
555 on the global carbon cycle (van der Werf et al., 2004). Global fire emissions of carbon reached
556 3.0 and 2.9 Pg C in 1997 and 1998 according to the GFED4s data. These two years produced the
557 largest source of fire-emitted carbon for the entire period 1997–2015. In comparison, global fire
558 emissions in 2015 reached 2.3 Pg C, close to the 1997–2015 average (2.2 Pg C yr⁻¹) but ~25%
559 lower than 1997–98 — the difference mainly occurring in the southern tropics (0–23.5°S, Fig.
560 S10). In particular, carbon emissions from deforestation and peat fires were two times lower in
561 2015 (0.6 Pg C) compared with 1997 (1.2 Pg C) (GFED4s data). Emissions from these fire types
562 are more likely to be a net carbon source, because they cannot be compensated by vegetation
563 regrowth within a short time. Fire emission data thus suggest a smaller contribution from fires to
564 AGR in 2015 than 1997–98.

565

566 There has been a long debate on whether tropical vegetation shows enhanced greenness as
567 indicated by vegetation indices (i.e., NDVI and enhanced vegetation index or EVI) during dry
568 seasons or drought periods in tropical forest (Bi et al., 2015; Huete et al., 2006; Morton et al.,
569 2014; Saleska et al., 2007; Samanta et al., 2010; Xu et al., 2011), and whether there is an
570 accompanying decrease in long-term vegetation productivity associated with droughts (Medlyn,
571 2011; Samanta et al., 2011; Zhao and Running, 2010). Some studies show enhanced green-up in

572 Amazonian forest during dry seasons mainly due to the release of radiation control on vegetation
573 activities (Bi et al., 2015; Huete et al., 2006; Myneni et al., 2007), while Morton et al. (2014)
574 argued that if errors of satellite observation angle are corrected, no increase in EVI can be
575 observed during dry seasons. Saleska et al. (2007) observed greener response of Amazonian
576 forest during a severe drought event, whereas Samanta et al. (2010) argued such observed green-
577 up is an artefact of atmosphere-corrupted data and the properly processed satellite observations
578 reveal browner Amazonian forests during the severe drought event. Subsequent studies by Bi et
579 al. (2016) and Xu et al. (2011) confirm the satellite-observed negative impacts of the drought
580 events.

581

582 While long-term forest plot data demonstrated consistent negative effect of droughts on tropical
583 carbon uptake mainly through enhanced tree mortality (Lewis et al., 2011; Phillips et al., 2009),
584 short-time site observations failed to reveal immediate reduction in forest net primary
585 productivity (Doughty et al., 2015) during drought, or reported even increased gross
586 photosynthesis or photosynthetic capacity when entering dry season (Huete et al., 2006; Wu et
587 al., 2016). Further, a large mortality event for trees will cause a legacy source over several years
588 rather than a rapid release of CO₂ to the atmosphere during the year when trees died. Therefore,
589 it remains challenging to reconcile immediate carbon uptake reduction on the occurrence of
590 drought in tropical ecosystems as diagnosed from atmospheric inversions (Gatti et al., 2014) and
591 the aforementioned findings from forest plot data. In dynamic global vegetation models
592 (DGVMs), the interannual variations of simulated land carbon sink are dominated by those in net
593 primary production (Wang et al., 2016), which contradicts the site-level observations by
594 Doughty et al. (2015).

595

596 Both Wang et al. (2013) and Wang et al. (2014) found a higher correlation coefficient between
597 interannual variability in tropical land carbon fluxes (as inferred from interannual variations in
598 AGR) with that in temperature than in precipitation, which is confirmed by our analysis of
599 inversion-based tropical land flux anomalies with climate variations (Fig. 4). However, forest
600 plot observations point to the prevailing drought as the dominant factor reducing forest carbon
601 storage (Phillips et al., 2009). The need thus remains to reconcile the findings of temperature
602 dominance at large spatial scale and precipitation/moisture dominance at fine scale. Recently,

603 Jung et al. (2017) suggested that the dominant role of soil moisture over land carbon flux
604 anomalies shifts to temperature when the scale of spatial aggregation increases, due to the
605 compensatory water effects in the process of spatial upscaling. We also find that for all seasons
606 except Q3, inversion-based land carbon uptake anomalies in the tropics and southern extratropics
607 are positively correlated with soil water content (data not shown), with 2015 having an extreme
608 low soil water content anomaly in Q4, echoing the extreme high temperature anomaly shown in
609 Fig. S4l. This might indicate that temperature impacts the land carbon uptake mainly by
610 increasing evaporative demand and decreasing soil water content.

611

612 **4.3 Data uncertainties and perspective**

613 On the global and hemispheric scales, the inversion-derived land- and ocean-atmosphere fluxes
614 are well constrained by the observed atmospheric CO₂ growth rates at measurement sites.
615 However, because the observational network is heterogeneous and sites are sparsely distributed
616 (Supplementary Material Fig. S11), land CO₂ fluxes cannot be resolved precisely over each grid
617 cell (Kaminski et al., 2001) and some regions are better constrained than others. This could
618 hinder the precise pixel-scale matching between gridded CO₂ flux maps and climate states or the
619 occurrence of climate extremes to investigate how climate extremes have affected carbon fluxes.
620 Although we have identified that carbon uptake transitions for some regions and seasons might
621 be related to certain climate extremes (e.g., the role of precipitation in TeNH of Q4 shown in Fig.
622 S5h), in general exact attribution of these transitions into different climate drivers could be
623 elusive. Further, a few other uncertainties matter for the specific objective of this study. First, the
624 atmospheric network increased over time, so that the inversions have a better ability to detect and
625 quantify a sharp transition in CO₂ fluxes occurring in the last than in the first decade of the
626 period analysed. This might hide the detection of other more extreme end-of-year carbon
627 transitions during early years of our target period (1981-2015). Second, because measurements
628 for early 2016 are not used in the CAMS inversion and are not completely available in the Jena
629 inversion, the constraining of the last season in 2015 is weaker than for the other three seasons.
630 This could influence estimating the exact magnitude of the extreme Q4 negative anomaly in land
631 carbon uptake in 2015. Third, the sparse network of sites in boreal Eurasia and the tropics might
632 diminish the ability of inversion systems to robustly allocation carbon fluxes spatially, which
633 could yield high uncertainty in the carbon fluxes diagnosed for these regions (van der Laan-

634 Luijkx et al., 2015; Stephens et al., 2007).

635

636 Despite these uncertainties, the strong transition of CO₂ fluxes from Q3 to Q4 is the largest ever
637 found in the inversion records analysed here. Although 2015 shows extreme greening in the
638 Northern Hemisphere, this strong greenness has been only translated into a moderate annual
639 carbon sink anomaly in 2015, because vegetation greenness and land uptake anomalies are
640 largely decoupled outside the growing season. The strong transition to a carbon source in TeNH
641 in Q4 is consistent with the high precipitation that might have led to a large increase in
642 respiration loss.

643

644 In the tropics, the transition to a strong source in TroSH in Q4 is congruent with the expected
645 response of ecosystems to the peak of an El Niño event. However, given the ambiguous findings
646 regarding changes in vegetation greenness during dry seasons or drought periods by previous
647 studies (Saleska et al., 2007; Xu et al., 2011), and the uncertain roles of climate variations in
648 driving the regional land carbon balance, more work is needed to reveal how these processes
649 have evolved during opposing ENSO phases (i.e., the cold phase of La Niña versus the warm
650 phase of El Niño). [Furthermore, large-scale spatial observation-based analysis is hampered by the scarcity of sites measuring atmospheric concentrations or land-atmosphere fluxes with the eddy covariance method \(Tramontana et al., 2016\).](#) For the boreal and temperate Northern
653 Hemisphere, further investigation is still needed to verify whether a coupling between strong
654 spring/summer uptake and autumn release is something intrinsic to natural ecosystems, or if
655 strong transitions to autumn release are triggered by some particular extreme climate shifts. [More detailed mechanisms can be explored by using long-term simultaneous observations of vegetation greenness and eddy covariance measurements of land-atmosphere fluxes combined with dynamic vegetation models.](#) Here, our results point to the need to better understand the
659 drivers of carbon dynamics at seasonal, or even shorter time scales at the regional to global level,
660 especially the link between such dynamics and climate extremes. Such understanding would help
661 us make better predictions of the response of the carbon cycle to multiple long-term drivers such
662 as atmospheric CO₂ growth and climate change.

663

664 **5 Conclusions**

665 We investigated the links among vegetation greenness, interannual land carbon flux variations
666 and climate variations for 1981–2015 using inversion-based land carbon flux data sets.
667 Consistent positive correlations between satellite-derived vegetation greenness and land carbon
668 uptakes are found for the Northern Hemisphere during the growing season, but outside the
669 growing season, vegetation greenness and land carbon uptake are largely decoupled. Carbon
670 uptake in the boreal Northern Hemisphere ($>45^{\circ}\text{N}$) is more consistently associated with
671 temperature than precipitation, although such a pattern is less evident for the temperate Northern
672 Hemisphere ($23.5\text{--}45^{\circ}\text{N}$). Consistent with previous studies, we found a strong negative impact
673 by temperature in the land carbon uptakes in the tropics and Southern Hemisphere, probably
674 driven by the role of temperature in soil water content that tends to induce drought conditions.

675

676 We put an emphasis on the seasonal dynamics of land carbon uptake in 2015. We found that
677 northern lands started with a higher-than-normal sink for the northern growing season, consistent
678 with enhanced vegetation greenness partly owing to elevated warming. However, this enhanced
679 sink was in part balanced by the carbon release in the autumn and winter, associated with
680 extremely high precipitation in Q4 in the temperate Northern Hemisphere ($23.5\text{--}45^{\circ}\text{N}$). [Our results emphasized the important role of the coupling between seasonal carbon dynamics in the annual net carbon balance of the land ecosystem. More research is needed on whether such a coupling, between enhanced spring and summer sink and reduced autumn uptake, is something intrinsic in northern ecosystems, and on the frequency and extent of its occurrence. The dominance of temperature in the boreal Northern Hemisphere \(\$>45^{\circ}\text{N}\$ \) and soil moisture in the temperate Northern Hemisphere \(\$23\text{--}45^{\circ}\text{N}\$ \) in their autumn carbon loss implies that future autumn temperature and precipitation change could have important consequences for the annual carbon balance of these regions. Hence, although continuing vegetation greening is projected mainly thanks to \$\text{CO}_2\$ fertilization \(Zhu et al., 2016\), such greening might not translate into enhanced land carbon uptake.](#)

691

692 For the tropics and Southern Hemisphere, a strong transition was found towards a large carbon
693 source for the last quarter of 2015, concomitant with the peak of El Niño development. This
694 strong transition of terrestrial CO_2 fluxes in the last season is the largest in the inversion records
695 since 1981, [even though annual fire emissions were \$\sim 25\%\$ lower than during El Niño of 1997–](#)

696 98. However, site-scale studies on tropical forest growth so far focusing on drought impacts
697 cannot provide an adequate explanation of such strong transitions. It is unclear how the
698 individual fluxes (gross primary production, net primary production, heterotrophic respiration)
699 that make up the land sink have responded to drought conditions. Our results point to the
700 possibility that, with more frequent extreme El Niño events being projected in the future, such
701 strong seasonal transitions in land carbon uptake might become more frequent and they can have
702 substantial impact on the capacity of land ecosystems to sequester carbon.

703 **References**

- 704 Adler, R. F., Huffman, G. J., Chang, A., Ferraro, R., Xie, P.-P., Janowiak, J., Rudolf, B.,
705 Schneider, U., Curtis, S., Bolvin, D., Gruber, A., Susskind, J., Arkin, P. and Nelkin, E.:
706 The Version-2 Global Precipitation Climatology Project (GPCP) Monthly Precipitation
707 Analysis (1979–Present), *J. Hydrometeorol.*, 4(6), 1147–1167, doi:10.1175/1525-
708 7541(2003)004<1147:TVGPCP>2.0.CO;2, 2003.
- 709 Ahlström, A., Raupach, M. R., Schurgers, G., Smith, B., Arneth, A., Jung, M., Reichstein, M.,
710 Canadell, J. G., Friedlingstein, P., Jain, A. K., Kato, E., Poulter, B., Sitch, S., Stocker, B.
711 D., Viovy, N., Wang, Y. P., Wiltshire, A., Zaehle, S. and Zeng, N.: The dominant role of
712 semi-arid ecosystems in the trend and variability of the land CO₂ sink, *Science*,
713 348(6237), 895–899, doi:10.1126/science.aaa1668, 2015.
- 714 Angert, A., Biraud, S., Bonfils, C., Henning, C. C., Buermann, W., Pinzon, J., Tucker, C. J. and
715 Fung, I.: Drier summers cancel out the CO₂ uptake enhancement induced by warmer
716 springs, *Proc. Natl. Acad. Sci. U. S. A.*, 102(31), 10823–10827,
717 doi:10.1073/pnas.0501647102, 2005.
- 718 Ballantyne, A. P., Alden, C. B., Miller, J. B., Tans, P. P. and White, J. W. C.: Increase in
719 observed net carbon dioxide uptake by land and oceans during the past 50 years, *Nature*,
720 488(7409), 70–72, doi:10.1038/nature11299, 2012.
- 721 Barichivich, J., Briffa, K. R., Myneni, R. B., Osborn, T. J., Melvin, T. M., Ciais, P., Piao, S. and
722 Tucker, C.: Large-scale variations in the vegetation growing season and annual cycle of
723 atmospheric CO₂ at high northern latitudes from 1950 to 2011, *Glob. Change Biol.*,
724 19(10), 3167–3183, doi:10.1111/gcb.12283, 2013.
- 725 Bastos, A., Ciais, P., Park, T., Zscheischler, J., Yue, C., Barichivich, J., Myneni, R. B., Peng, S.,
726 Piao, S. and Zhu, Z.: Was the extreme Northern Hemisphere greening in 2015
727 predictable?, *Environ. Res. Lett.*, 12(4), 044016, doi:10.1088/1748-9326/aa67b5, 2017.
- 728 Bi, J., Knyazikhin, Y., Choi, S., Park, T., Barichivich, J., Ciais, P., Fu, R., Sangram Ganguly,
729 Hall, F., Hilker, T., Huete, A., Jones, M., Kimball, J., Lyapustin, A. I., Matti Möttöus,
730 Nemani, R. R., Piao, S., Poulter, B., Saleska, S. R., Saatchi, S. S., Liang Xu, Zhou, L. and
731 Myneni, R. B.: Sunlight mediated seasonality in canopy structure and photosynthetic
732 activity of Amazonian rainforests, *Environ. Res. Lett.*, 10(6), 064014, doi:10.1088/1748-
733 9326/10/6/064014, 2015.
- 734 Bi, J., Myneni, R., Lyapustin, A., Wang, Y., Park, T., Chi, C., Yan, K. and Knyazikhin, Y.:
735 Amazon forests' response to droughts: A perspective from the MAIAC product. *Remote*
736 *Sens.*, 8(4), 356, doi:10.3390/rs8040356, 2016.
- 737 Cai, W., Borlace, S., Lengaigne, M., van Rensch, P., Collins, M., Vecchi, G., Timmermann, A.,
738 Santoso, A., McPhaden, M. J., Wu, L., England, M. H., Wang, G., Guilyardi, E. and Jin,
739 F.-F.: Increasing frequency of extreme El Niño events due to greenhouse warming, *Nat.*
740 *Clim. Change*, 4(2), 111–116, doi:10.1038/nclimate2100, 2014.
- 741 Canadell, J. G., Le Quéré, C., Raupach, M. R., Field, C. B., Buitenhuis, E. T., Ciais, P., Conway,
742 T. J., Gillett, N. P., Houghton, R. A. and Marland, G.: Contributions to accelerating
743 atmospheric CO₂ growth from economic activity, carbon intensity, and efficiency of
744 natural sinks, *Proc. Natl. Acad. Sci.*, 104(47), 18866–18870, 2007.
- 745 Chen, J., Jönsson, P., Tamura, M., Gu, Z., Matsushita, B. and Eklundh, L.: A simple method for
746 reconstructing a high-quality NDVI time-series data set based on the Savitzky–Golay
747 filter, *Remote Sens. Environ.*, 91(3), 332–344, doi:10.1016/j.rse.2004.03.014, 2004.
- 748 Chevallier, F., Fisher, M., Peylin, P., Serraz, S., Bousquet, P., Bréon, F.-M., Chédin, A. and

749 Ciais, P.: Inferring CO₂ sources and sinks from satellite observations: Method and
750 application to TOVS data, *J. Geophys. Res. Atmospheres*, 110(D24), D24309,
751 doi:10.1029/2005JD006390, 2005.

752 Chevallier, F., Ciais, P., Conway, T. J., Aalto, T., Anderson, B. E., Bousquet, P., Brunke, E. G.,
753 Ciattaglia, L., Esaki, Y., Fröhlich, M., Gomez, A., Gomez-Pelaez, A. J., Haszpra, L.,
754 Krummel, P. B., Langenfelds, R. L., Leuenberger, M., Machida, T., Maignan, F.,
755 Matsueda, H., Morguí, J. A., Mukai, H., Nakazawa, T., Peylin, P., Ramonet, M., Rivier,
756 L., Sawa, Y., Schmidt, M., Steele, L. P., Vay, S. A., Vermeulen, A. T., Wofsy, S. and
757 Worthy, D.: CO₂ surface fluxes at grid point scale estimated from a global 21 year
758 reanalysis of atmospheric measurements, *J. Geophys. Res. Atmospheres*, 115(D21),
759 D21307, doi:10.1029/2010JD013887, 2010.

760 Cox, P. M., Pearson, D., Booth, B. B., Friedlingstein, P., Huntingford, C., Jones, C. D. and Luke,
761 C. M.: Sensitivity of tropical carbon to climate change constrained by carbon dioxide
762 variability, *Nature*, 494(7437), 341–344, doi:10.1038/nature11882, 2013.

763 Dee, D. P., Uppala, S. M., Simmons, A. J., Berrisford, P., Poli, P., Kobayashi, S., Andrae, U.,
764 Balmaseda, M. A., Balsamo, G., Bauer, P., Bechtold, P., Beljaars, A. C. M., van de Berg,
765 L., Bidlot, J., Bormann, N., Delsol, C., Dragani, R., Fuentes, M., Geer, A. J., Haimberger,
766 L., Healy, S. B., Hersbach, H., Hólm, E. V., Isaksen, I., Kållberg, P., Köhler, M.,
767 Matricardi, M., McNally, A. P., Monge-Sanz, B. M., Morcrette, J.-J., Park, B.-K.,
768 Peubey, C., de Rosnay, P., Tavolato, C., Thépaut, J.-N. and Vitart, F.: The ERA-Interim
769 reanalysis: configuration and performance of the data assimilation system, *Q. J. R.*
770 *Meteorol. Soc.*, 137(656), 553–597, doi:10.1002/qj.828, 2011.

771 Didan K 2015 MOD13C1 MODIS/Terra Vegetation Indices 16-Day L3 Global 0.05Deg CMG
772 V006 NASA EOSDIS Land Processes DAAC ([https://doi.org/10.5067/MODIS/
773 MOD13C1.006](https://doi.org/10.5067/MODIS/MOD13C1.006))

774 Doughty, C. E., Metcalfe, D. B., Girardin, C. a. J., Amézquita, F. F., Cabrera, D. G., Huasco, W.
775 H., Silva-Espejo, J. E., Araujo-Murakami, A., da Costa, M. C., Rocha, W., Feldpausch,
776 T. R., Mendoza, A. L. M., da Costa, A. C. L., Meir, P., Phillips, O. L. and Malhi, Y.:
777 Drought impact on forest carbon dynamics and fluxes in Amazonia, *Nature*, 519(7541),
778 78–82, doi:10.1038/nature14213, 2015.

779 Field, R. D., Werf, G. R. van der, Fanin, T., Fetzer, E. J., Fuller, R., Jethva, H., Levy, R.,
780 Livesey, N. J., Luo, M., Torres, O. and Worden, H. M.: Indonesian fire activity and
781 smoke pollution in 2015 show persistent nonlinear sensitivity to El Niño-induced
782 drought, *Proc. Natl. Acad. Sci.*, 113(33), 9204–9209, doi:10.1073/pnas.1524888113,
783 2016.

784 Forkel, M., Carvalhais, N., Rödenbeck, C., Keeling, R., Heimann, M., Thonicke, K., Zaehle, S.
785 and Reichstein, M.: Enhanced seasonal CO₂ exchange caused by amplified plant
786 productivity in northern ecosystems, *Science*, 351(6274), 696–699,
787 doi:10.1126/science.aac4971, 2016.

788 Gamon, J. A., Field, C. B., Goulden, M. L., Griffin, K. L., Hartley, A. E., Joel, G., Peñuelas, J.
789 and Valentini, R.: Relationships Between NDVI, Canopy Structure, and Photosynthesis
790 in Three Californian Vegetation Types, *Ecol. Appl.*, 5(1), 28–41, doi:10.2307/1942049,
791 1995.

792 Gatti, L. V., Gloor, M., Miller, J. B., Doughty, C. E., Malhi, Y., Domingues, L. G., Basso, L. S.,
793 Martinewski, A., Correia, C. S. C., Borges, V. F., Freitas, S., Braz, R., Anderson, L. O.,
794 Rocha, H., Grace, J., Phillips, O. L. and Lloyd, J.: Drought sensitivity of Amazonian

795 carbon balance revealed by atmospheric measurements, *Nature*, 506(7486), 76–80,
796 doi:10.1038/nature12957, 2014.

797 Graven, H. D., Keeling, R. F., Piper, S. C., Patra, P. K., Stephens, B. B., Wofsy, S. C., Welp, L.
798 R., Sweeney, C., Tans, P. P., Kelley, J. J., Daube, B. C., Kort, E. A., Santoni, G. W. and
799 Bent, J. D.: Enhanced Seasonal Exchange of CO₂ by Northern Ecosystems Since 1960,
800 *Science*, 341(6150), 1085–1089, doi:10.1126/science.1239207, 2013.

801 Gu, L., Baldocchi, D. D., Wofsy, S. C., Munger, J. W., Michalsky, J. J., Urbanski, S. P. and
802 Boden, T. A.: Response of a Deciduous Forest to the Mount Pinatubo Eruption:
803 Enhanced Photosynthesis, *Science*, 299(5615), 2035–2038, doi:10.1126/science.1078366,
804 2003.

805 Hadden, D. and Grelle, A.: Changing temperature response of respiration turns boreal forest
806 from carbon sink into carbon source, *Agric. For. Meteorol.*, 223, 30–38,
807 doi:10.1016/j.agrformet.2016.03.020, 2016.

808 Huete, A. R., Didan, K., Shimabukuro, Y. E., Ratana, P., Saleska, S. R., Hutyrá, L. R., Yang, W.,
809 Nemani, R. R. and Myneni, R.: Amazon rainforests green-up with sunlight in dry season,
810 *Geophys. Res. Lett.*, 33(6), L06405, doi:10.1029/2005GL025583, 2006.

811 Huijnen, V., Wooster, M. J., Kaiser, J. W., Gaveau, D. L. A., Flemming, J., Parrington, M.,
812 Inness, A., Murdiyarso, D., Main, B. and Weele, M. van: Fire carbon emissions over
813 maritime southeast Asia in 2015 largest since 1997, *Sci. Rep.*, 6, 26886,
814 doi:10.1038/srep26886, 2016.

815 Jacobson, A. R., Mikaloff Fletcher, S. E., Gruber, N., Sarmiento, J. L. and Gloor, M.: A joint
816 atmosphere-ocean inversion for surface fluxes of carbon dioxide: 1. Methods and global-
817 scale fluxes, *Glob. Biogeochem. Cycles*, 21(1), GB1019, doi:10.1029/2005GB002556,
818 2007.

819 Jiménez-Muñoz, J. C., Mattar, C., Barichivich, J., Santamaría-Artigas, A., Takahashi, K., Malhi,
820 Y., Sobrino, J. A. and Schrier, G. van der: Record-breaking warming and extreme
821 drought in the Amazon rainforest during the course of El Niño 2015–2016, *Sci. Rep.*, 6,
822 33130, doi:10.1038/srep33130, 2016.

823 Jönsson, P. and Eklundh, L.: TIMESAT—a program for analyzing time-series of satellite sensor
824 data, *Comput. Geosci.*, 30(8), 833–845, doi:10.1016/j.cageo.2004.05.006, 2004.

825 Jung, M., Reichstein, M., Schwalm, C. R., Huntingford, C., Sitch, S., Ahlström, A., Arneth, A.,
826 Camps-Valls, G., Ciais, P., Friedlingstein, P. and others: Compensatory water effects link
827 yearly global land CO₂ sink changes to temperature, *Nature* [online] Available from:
828 <https://www.nature.com/nature/journal/vaop/ncurrent/full/nature20780.html> (Accessed
829 19 June 2017), 2017.

830 Kaminski, T., Rayner, P. J., Heimann, M. and Enting, I. G.: On aggregation errors in
831 atmospheric transport inversions, *J. Geophys. Res. Atmospheres*, 106(D5), 4703–4715,
832 doi:10.1029/2000JD900581, 2001.

833 van der Laan-Luijkx, I. T., van der Velde, I. R., Krol, M. C., Gatti, L. V., Domingues, L. G.,
834 Correia, C. S. C., Miller, J. B., Gloor, M., van Leeuwen, T. T., Kaiser, J. W.,
835 Wiedinmyer, C., Basu, S., Clerbaux, C. and Peters, W.: Response of the Amazon carbon
836 balance to the 2010 drought derived with CarbonTracker South America, *Glob. Biogeochem. Cycles*, 29(7), 2014GB005082, doi:10.1002/2014GB005082, 2015.

837 Lewis, S. L., Brando, P. M., Phillips, O. L., van der Heijden, G. M. and Nepstad, D.: The 2010
838 amazon drought, *Science*, 331(6017), 554–554, 2011.

839 Li, W., Ciais, P., Wang, Y., Peng, S., Broquet, G., Ballantyne, A. P., Canadell, J. G., Cooper, L.,

841 Friedlingstein, P., Quéré, C. L., Myneni, R. B., Peters, G. P., Piao, S. and Pongratz, J.:
842 Reducing uncertainties in decadal variability of the global carbon budget with multiple
843 datasets, *Proc. Natl. Acad. Sci.*, 113(46), 13104–13108, doi:10.1073/pnas.1603956113,
844 2016.

845 Medlyn, B. E.: Comment on “Drought-Induced Reduction in Global Terrestrial Net Primary
846 Production from 2000 Through 2009,” *Science*, 333(6046), 1093–1093,
847 doi:10.1126/science.1199544, 2011.

848 Morton, D. C., Nagol, J., Carabajal, C. C., Rosette, J., Palace, M., Cook, B. D., Vermote, E. F.,
849 Harding, D. J. and North, P. R. J.: Amazon forests maintain consistent canopy structure
850 and greenness during the dry season, *Nature*, 506(7487), 221–224,
851 doi:10.1038/nature13006, 2014.

852 Myneni, R. B., Keeling, C. D., Tucker, C. J., Asrar, G. and Nemani, R. R.: Increased plant
853 growth in the northern high latitudes from 1981 to 1991, *Nature*, 386(6626), 698–702,
854 doi:10.1038/386698a0, 1997.

855 Myneni, R. B., Yang, W., Nemani, R. R., Huete, A. R., Dickinson, R. E., Knyazikhin, Y., Didan,
856 K., Fu, R., Juárez, R. I. N., Saatchi, S. S., Hashimoto, H., Ichii, K., Shabanov, N. V., Tan,
857 B., Ratana, P., Privette, J. L., Morisette, J. T., Vermote, E. F., Roy, D. P., Wolfe, R. E.,
858 Friedl, M. A., Running, S. W., Votava, P., El-Saleous, N., Devadiga, S., Su, Y. and
859 Salomonson, V. V.: Large seasonal swings in leaf area of Amazon rainforests, *Proc. Natl.*
860 *Acad. Sci.*, 104(12), 4820–4823, doi:10.1073/pnas.0611338104, 2007.

861 Nemani, R. R., Keeling, C. D., Hashimoto, H., Jolly, W. M., Piper, S. C., Tucker, C. J., Myneni,
862 R. B. and Running, S. W.: Climate-Driven Increases in Global Terrestrial Net Primary
863 Production from 1982 to 1999, *Science*, 300(5625), 1560–1563,
864 doi:10.1126/science.1082750, 2003.

865 Orth, R., Zscheischler, J. and Seneviratne, S. I.: Record dry summer in 2015 challenges
866 precipitation projections in Central Europe, *Sci. Rep.*, 6, 28334, doi:10.1038/srep28334,
867 2016.

868 Phillips, O. L., Aragão, L. E. O. C., Lewis, S. L., Fisher, J. B., Lloyd, J., López-González, G.,
869 Malhi, Y., Monteagudo, A., Peacock, J., Quesada, C. A., Heijden, G. van der, Almeida,
870 S., Amaral, I., Arroyo, L., Aymard, G., Baker, T. R., Bánki, O., Blanc, L., Bonal, D.,
871 Brando, P., Chave, J., Oliveira, Á. C. A. de, Cardozo, N. D., Czimczik, C. I., Feldpausch,
872 T. R., Freitas, M. A., Gloor, E., Higuchi, N., Jiménez, E., Lloyd, G., Meir, P., Mendoza,
873 C., Morel, A., Neill, D. A., Nepstad, D., Patiño, S., Peñuela, M. C., Prieto, A., Ramírez,
874 F., Schwarz, M., Silva, J., Silveira, M., Thomas, A. S., Steege, H. ter, Stropp, J.,
875 Vásquez, R., Zelazowski, P., Dávila, E. A., Andelman, S., Andrade, A., Chao, K.-J.,
876 Erwin, T., Fiore, A. D., C. E. H., Keeling, H., Killeen, T. J., Laurance, W. F., Cruz, A. P.,
877 Pitman, N. C. A., Vargas, P. N., Ramírez-Angulo, H., Rudas, A., Salamão, R., Silva, N.,
878 Terborgh, J. and Torres-Lezama, A.: Drought Sensitivity of the Amazon Rainforest,
879 *Science*, 323(5919), 1344–1347, doi:10.1126/science.1164033, 2009.

880 Piao, S., Ciais, P., Friedlingstein, P., Peylin, P., Reichstein, M., Luysaert, S., Margolis, H.,
881 Fang, J., Barr, A., Chen, A., Grelle, A., Hollinger, D. Y., Laurila, T., Lindroth, A.,
882 Richardson, A. D. and Vesala, T.: Net carbon dioxide losses of northern ecosystems in
883 response to autumn warming, *Nature*, 451(7174), 49–52, doi:10.1038/nature06444, 2008.

884 Poulter, B., Frank, D., Ciais, P., Myneni, R. B., Andela, N., Bi, J., Broquet, G., Canadell, J. G.,
885 Chevallier, F., Liu, Y. Y., Running, S. W., Sitch, S. and van der Werf, G. R.:
886 Contribution of semi-arid ecosystems to interannual variability of the global carbon

887 cycle, *Nature*, 509(7502), 600–603, doi:10.1038/nature13376, 2014.

888 Prather, M. J., Holmes, C. D. and Hsu, J.: Reactive greenhouse gas scenarios: Systematic
889 exploration of uncertainties and the role of atmospheric chemistry, *Geophys. Res. Lett.*,
890 39(9), L09803, doi:10.1029/2012GL051440, 2012.

891 Quéré, C. L., Andrew, R. M., Canadell, J. G., Sitch, S., Korsbakken, J. I., Peters, G. P., Manning,
892 A. C., Boden, T. A., Tans, P. P., Houghton, R. A., Keeling, R. F., Alin, S., Andrews, O.
893 D., Anthoni, P., Barbero, L., Bopp, L., Chevallier, F., Chini, L. P., Ciais, P., Currie, K.,
894 Delire, C., Doney, S. C., Friedlingstein, P., Gkritzalis, T., Harris, I., Hauck, J., Haverd,
895 V., Hoppema, M., Klein Goldewijk, K., Jain, A. K., Kato, E., Körtzinger, A.,
896 Landschützer, P., Lefèvre, N., Lenton, A., Lienert, S., Lombardozi, D., Melton, J. R.,
897 Metzl, N., Millero, F., Monteiro, P. M. S., Munro, D. R., Nabel, J. E. M. S., Nakaoka, S.,
898 O'Brien, K., Olsen, A., Omar, A. M., Ono, T., Pierrot, D., Poulter, B., Rödenbeck, C.,
899 Salisbury, J., Schuster, U., Schwinger, J., Séférian, R., Skjelvan, I., Stocker, B. D.,
900 Sutton, A. J., Takahashi, T., Tian, H., Tilbrook, B., Laan-Luijkx, I. T. van der, Werf, G.
901 R. van der, Viovy, N., Walker, A. P., Wiltshire, A. J. and Zaehle, S.: Global Carbon
902 Budget 2016, *Earth Syst. Sci. Data*, 8(2), 605–649, doi:10.5194/essd-8-605-2016, 2016.

903 Rödenbeck, C.: Estimating CO₂ sources and sinks from atmospheric mixing ratio measurements
904 using a global inversion of atmospheric transport, Max Planck Institute for
905 Biogeochemistry, 2005.

906 Rödenbeck, C., Houweling, S., Gloor, M. and Heimann, M.: CO₂ flux history 1982–2001
907 inferred from atmospheric data using a global inversion of atmospheric transport, *Atmos*
908 *Chem Phys*, 3(6), 1919–1964, doi:10.5194/acp-3-1919-2003, 2003.

909 Saleska, S. R., Didan, K., Huete, A. R. and Rocha, H. R. da: Amazon Forests Green-Up During
910 2005 Drought, *Science*, 318(5850), 612–612, doi:10.1126/science.1146663, 2007.

911 Samanta, A., Ganguly, S., Hashimoto, H., Devadiga, S., Vermote, E., Knyazikhin, Y., Nemani,
912 R. R. and Myneni, R. B.: Amazon forests did not green-up during the 2005 drought,
913 *Geophys. Res. Lett.*, 37(5), L05401, doi:10.1029/2009GL042154, 2010.

914 Samanta, A., Costa, M. H., Nunes, E. L., Vieira, S. A., Xu, L. and Myneni, R. B.: Comment on
915 “Drought-Induced Reduction in Global Terrestrial Net Primary Production from 2000
916 Through 2009,” *Science*, 333(6046), 1093–1093, doi:10.1126/science.1199048, 2011.

917 Stephens, B. B., Gurney, K. R., Tans, P. P., Sweeney, C., Peters, W., Bruhwiler, L., Ciais, P.,
918 Ramonet, M., Bousquet, P., Nakazawa, T., Aoki, S., Machida, T., Inoue, G.,
919 Vinnichenko, N., Lloyd, J., Jordan, A., Heimann, M., Shibistova, O., Langenfelds, R. L.,
920 Steele, L. P., Francey, R. J. and Denning, A. S.: Weak Northern and Strong Tropical
921 Land Carbon Uptake from Vertical Profiles of Atmospheric CO₂, *Science*, 316(5832),
922 1732–1735, doi:10.1126/science.1137004, 2007.

923 Tanja, S., Berninger, F., Vesala, T., Markkanen, T., Hari, P., Mäkelä, A., Ilvesniemi, H.,
924 Hänninen, H., Nikinmaa, E., Huttula, T., Laurila, T., Aurela, M., Grelle, A., Lindroth, A.,
925 Arneth, A., Shibistova, O. and Lloyd, J.: Air temperature triggers the recovery of
926 evergreen boreal forest photosynthesis in spring, *Glob. Change Biol.*, 9(10), 1410–1426,
927 doi:10.1046/j.1365-2486.2003.00597.x, 2003.

928 Tramontana, G., Jung, M., Schwalm, C. R., Ichii, K., Camps-Valls, G., Ráduly, B., Reichstein,
929 M., Arain, M. A., Cescatti, A., Kiely, G., Merbold, L., Serrano-Ortiz, P., Sickert, S.,
930 Wolf, S. and Papale, D.: Predicting carbon dioxide and energy fluxes across global
931 FLUXNET sites with regression algorithms, *Biogeosciences*, 13(14), 4291–4313,
932 doi:10.5194/bg-13-4291-2016, 2016.

- 933 Ueyama, M., Iwata, H. and Harazono, Y.: Autumn warming reduces the CO₂ sink of a black
934 spruce forest in interior Alaska based on a nine-year eddy covariance measurement, *Glob.*
935 *Change Biol.*, 20(4), 1161–1173, doi:10.1111/gcb.12434, 2014.
- 936 Wang, J., Zeng, N. and Wang, M.: Interannual variability of the atmospheric CO₂ growth rate:
937 roles of precipitation and temperature, *Biogeosciences*, 13(8), 2339–2352,
938 doi:10.5194/bg-13-2339-2016, 2016.
- 939 Wang, W., Ciais, P., Nemani, R. R., Canadell, J. G., Piao, S., Sitch, S., White, M. A., Hashimoto,
940 H., Milesi, C. and Myneni, R. B.: Variations in atmospheric CO₂ growth rates coupled
941 with tropical temperature, *Proc. Natl. Acad. Sci.*, 110(32), 13061–13066,
942 doi:10.1073/pnas.1219683110, 2013.
- 943 Wang, X., Piao, S., Ciais, P., Friedlingstein, P., Myneni, R. B., Cox, P., Heimann, M., Miller, J.,
944 Peng, S., Wang, T., Yang, H. and Chen, A.: A two-fold increase of carbon cycle
945 sensitivity to tropical temperature variations, *Nature*, 506(7487), 212–215,
946 doi:10.1038/nature12915, 2014.
- 947 van der Werf, G. R., Randerson, J. T., Collatz, G. J., Giglio, L., Kasibhatla, P. S., Arellano, A.
948 F., Olsen, S. C. and Kasischke, E. S.: Continental-Scale Partitioning of Fire Emissions
949 During the 1997 to 2001 El Niño/La Niña Period, *Science*, 303(5654), 73–76,
950 doi:10.1126/science.1090753, 2004.
- 951 van der Werf, G. R., Dempewolf, J., Trigg, S. N., Randerson, J. T., Kasibhatla, P. S., Giglio, L.,
952 Murdiyarso, D., Peters, W., Morton, D. C., Collatz, G. J., Dolman, A. J. and DeFries, R.
953 S.: Climate regulation of fire emissions and deforestation in equatorial Asia, *Proc. Natl.*
954 *Acad. Sci. U. S. A.*, 105(51), 20350–20355, doi:10.1073/pnas.0803375105, 2008.
- 955 Wolf, S., Keenan, T. F., Fisher, J. B., Baldocchi, D. D., Desai, A. R., Richardson, A. D., Scott,
956 R. L., Law, B. E., Litvak, M. E., Brunsell, N. A., Peters, W. and Laan-Luijckx, I. T. van
957 der: Warm spring reduced carbon cycle impact of the 2012 US summer drought, *Proc.*
958 *Natl. Acad. Sci.*, 113(21), 5880–5885, doi:10.1073/pnas.1519620113, 2016.
- 959 Wolter, K. and Timlin, M. S.: El Niño/Southern Oscillation behaviour since 1871 as diagnosed
960 in an extended multivariate ENSO index (MEI.ext), *Int. J. Climatol.*, 31(7), 1074–1087,
961 doi:10.1002/joc.2336, 2011.
- 962 Wu, J., Albert, L. P., Lopes, A. P., Restrepo-Coupe, N., Hayek, M., Wiedemann, K. T., Guan,
963 K., Stark, S. C., Christoffersen, B., Prohaska, N., Tavares, J. V., Marostica, S.,
964 Kobayashi, H., Ferreira, M. L., Campos, K. S., Silva, R. da, Brando, P. M., Dye, D. G.,
965 Huxman, T. E., Huete, A. R., Nelson, B. W. and Saleska, S. R.: Leaf development and
966 demography explain photosynthetic seasonality in Amazon evergreen forests, *Science*,
967 351(6276), 972–976, doi:10.1126/science.aad5068, 2016.
- 968 Xu, L., Samanta, A., Costa, M. H., Ganguly, S., Nemani, R. R. and Myneni, R. B.: Widespread
969 decline in greenness of Amazonian vegetation due to the 2010 drought, *Geophys. Res.*
970 *Lett.*, 38(7), L07402, doi:10.1029/2011GL046824, 2011.
- 971 Yin, Y., Ciais, P., Chevallier, F., van der Werf, G. R., Fanin, T., Broquet, G., Boesch, H., Cozic,
972 A., Hauglustaine, D., Szopa, S. and Wang, Y.: Variability of fire carbon emissions in
973 equatorial Asia and its nonlinear sensitivity to El Niño, *Geophys. Res. Lett.*,
974 2016GL070971, doi:10.1002/2016GL070971, 2016.
- 975 Zhao, M. and Running, S. W.: Drought-Induced Reduction in Global Terrestrial Net Primary
976 Production from 2000 Through 2009, *Science*, 329(5994), 940–943,
977 doi:10.1126/science.1192666, 2010.
- 978 Zhou, L., Tucker, C. J., Kaufmann, R. K., Slayback, D., Shabanov, N. V. and Myneni, R. B.:

979 Variations in northern vegetation activity inferred from satellite data of vegetation index
980 during 1981 to 1999, *J. Geophys. Res. Atmospheres*, 106(D17), 20069–20083,
981 doi:10.1029/2000JD000115, 2001.

982 Zhu, Z., Piao, S., Myneni, R. B., Huang, M., Zeng, Z., Canadell, J. G., Ciais, P., Sitch, S.,
983 Friedlingstein, P., Arneth, A., Cao, C., Cheng, L., Kato, E., Koven, C., Li, Y., Lian, X.,
984 Liu, Y., Liu, R., Mao, J., Pan, Y., Peng, S., Peñuelas, J., Poulter, B., Pugh, T. A. M.,
985 Stocker, B. D., Viovy, N., Wang, X., Wang, Y., Xiao, Z., Yang, H., Zaehle, S. and Zeng,
986 N.: Greening of the Earth and its drivers, *Nat. Clim. Change*, 6(8), 791–795,
987 doi:10.1038/nclimate3004, 2016.

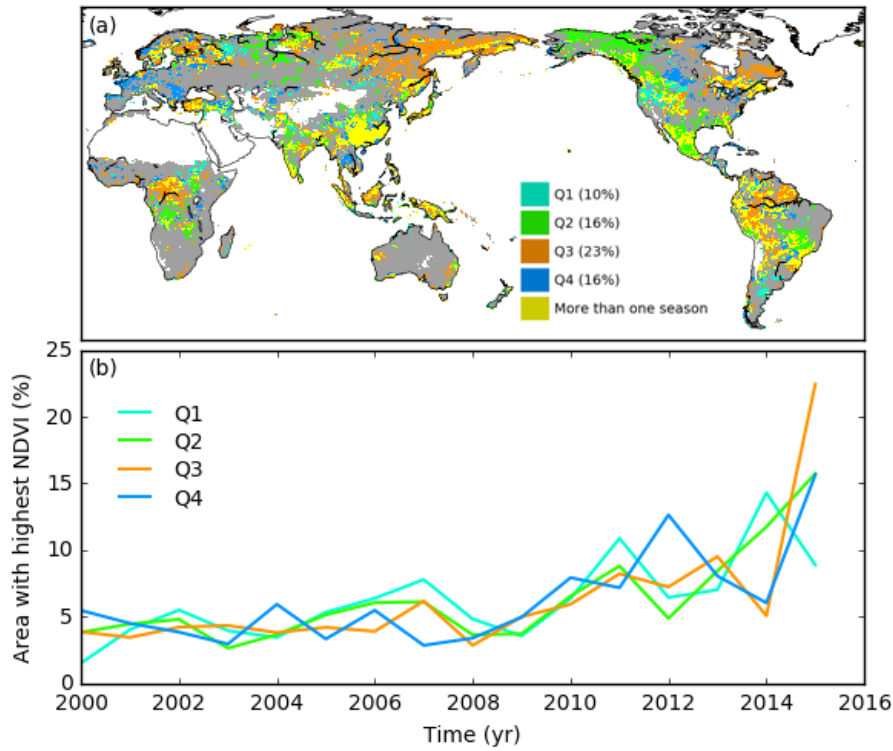
988 **Acknowledgements**

990 C.Y. and P.C. acknowledge funding from the European Commission's 7th Framework
991 Programme, under grant agreement number 603542 (LUC4C). The work of F.C. was funded by
992 the Copernicus Atmosphere Monitoring Service, implemented by the European Centre for
993 Medium-Range Weather Forecasts (ECMWF) on behalf of the European Commission. Taejin
994 Park was supported by the NASA Earth and Space Science Fellowship Program (grant no.
995 NNX16AO34H). We thank all the scientists involved in the surface and aircraft measurement of
996 atmospheric CO₂ concentration and in archiving these data and making them available. We also
997 thank Dr. Matthias Forkel and the anonymous reviewer for their comments that helped improve
998 the quality of the manuscript. We thank Mr. John Gash for improving the English of our
999 manuscript.

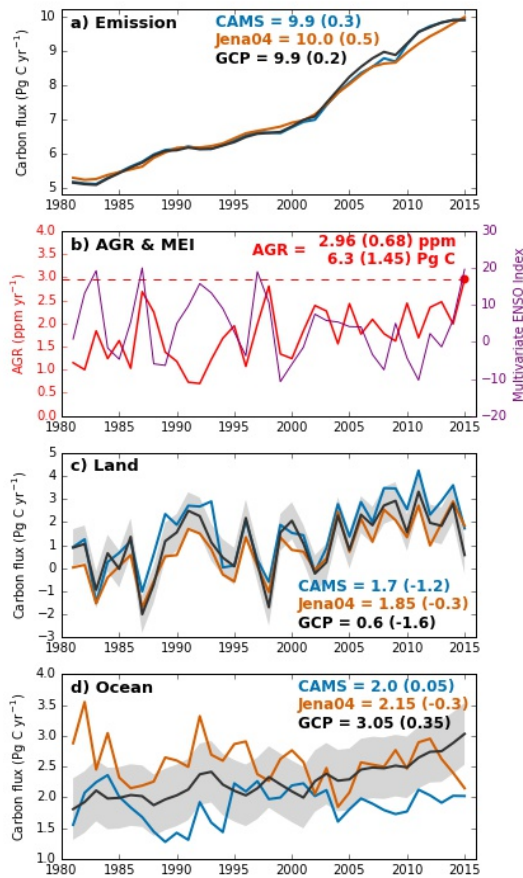
1000

1001 **Author contributions**

1002 P.C., F.C., C.Y. and A.B. conceived the study. C.Y. performed the analysis and made the first
1003 draft. F.C. and C.R. provided the inversion data. T. P. provided the NDVI data. All authors
1004 contributed to the interpretation of the results and writing of the paper.



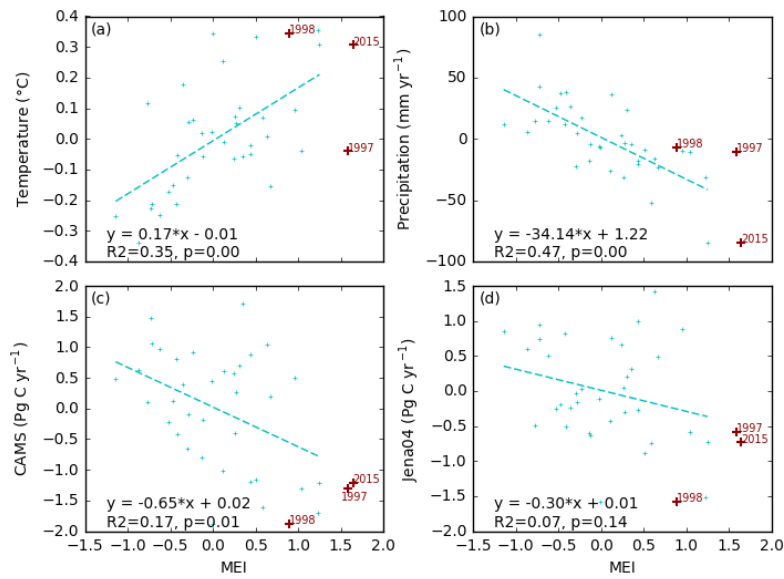
1005
 1006 **Figure 1** Year 2015 as the greenest year over the period 2000-2015. (a) Distribution of seasons
 1007 for which 2015 NDVI ranks the highest during the period 2000-2015. Yellow-coloured pixels
 1008 indicate grid cells where 2015 NDVI ranks highest for more than one season. For each season,
 1009 the fraction of global vegetated land area for which 2015 NDVI ranks highest is shown in the
 1010 inset colour scale. (b) Temporal evolution of the percentage of vegetated land with highest NDVI
 1011 over 2000-2015 for each season and different years. The sum total of vertical-axis values for
 1012 each season over all years is 100%. Q1 = January–March; Q2 = April–June; Q3 = July–
 1013 September; Q4 = October–December.



1014

1015 **Figure 2** Global carbon fluxes and atmospheric CO₂ growth rates for 1981–2015. (a) Carbon
 1016 emissions from fossil fuel and industry used in the CAMS (blue) and Jena04 (orange) inversions,
 1017 (b) annual atmospheric CO₂ growth rate (AGR, in red) from NOAA/ESRL linked to Multivariate
 1018 ENSO Index (in purple), and (c) land and (d) ocean carbon sinks for 1981–2015. Emissions, land
 1019 and ocean carbon sinks from the Global Carbon Project (GCP, in black) are also shown for
 1020 comparison. In subplots (c) and (d), a carbon flux of 0.45 Pg C yr⁻¹ was used to correct
 1021 inversion-derived land and ocean sinks to account for pre-industrial land-to-ocean carbon flux as
 1022 in Le Quéré et al. (2016). All numbers indicate values in 2015 (Pg C yr⁻¹, rounded to ±0.05 Pg C
 1023 yr⁻¹), with those in brackets showing linearly de-trended anomalies for the same year.

1024

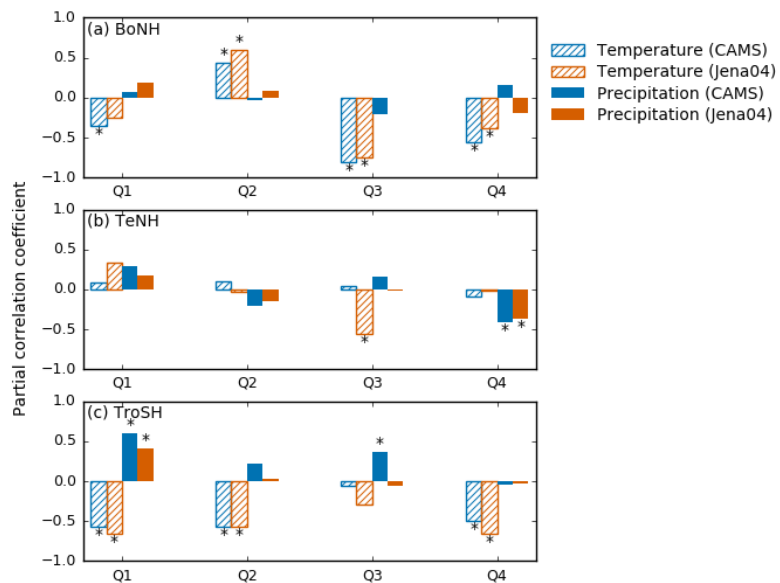


1025

1026 **Figure 3** Relationships between anomalies of (a) land air temperature, (b) land precipitation, (c)
1027 land carbon fluxes by the CAMS inversion, (d) land carbon fluxes by the Jena04 inversion, and
1028 the Multivariate ENSO Index (MEI). All variables are linearly de-trended over 1981–2015.

1029

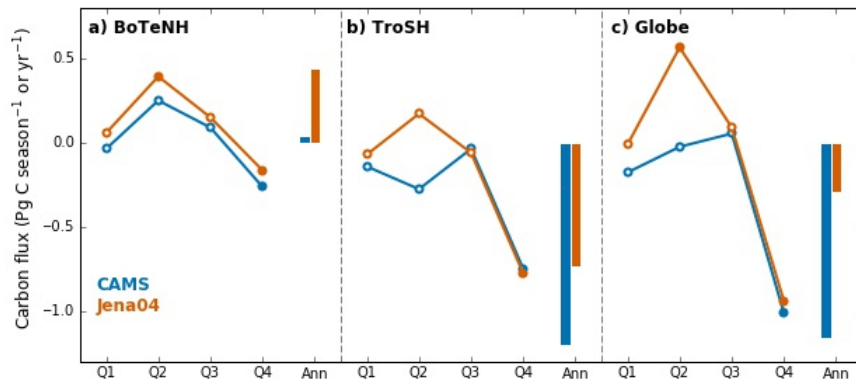
1030



1031

1032

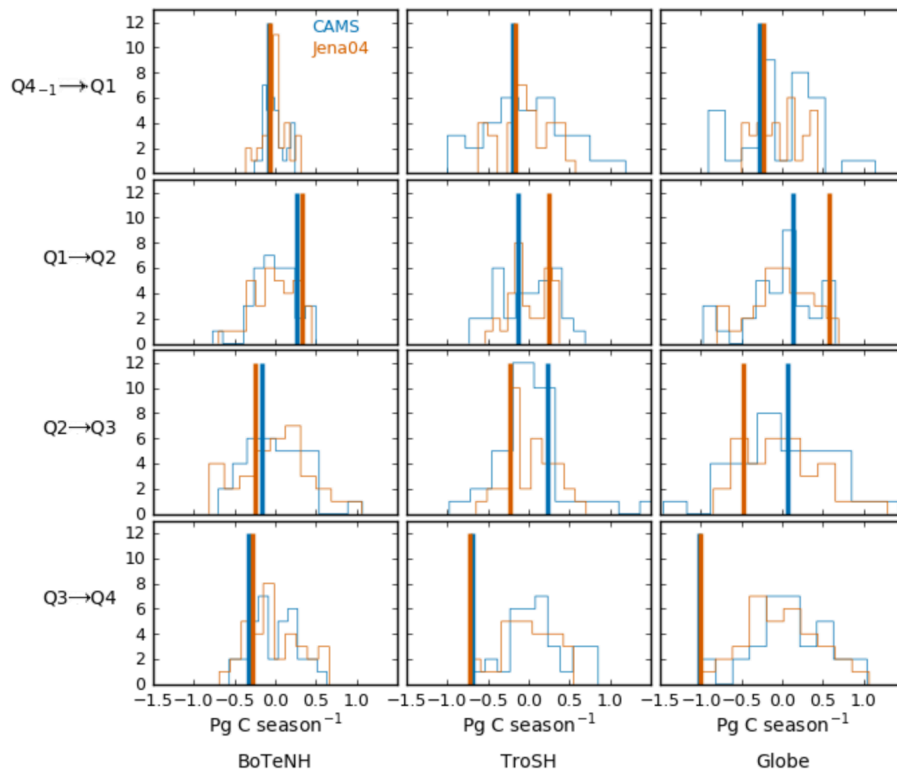
1033 **Figure 4** Partial correlation coefficients of de-trended annual anomalies of land carbon fluxes by
1034 CAMS and Jena04 inversions against the anomalies in temperature and precipitation of different
1035 seasons. n = 34. An asterisk indicates significant correlation ($p < 0.05$).



1036

1037 **Figure 5** Seasonal land carbon uptake anomalies in 2015. Data are linearly de-trended over
 1038 1981-2015 for different seasons in 2015, by CAMS (blue) and Jena04 (orange) inversion data.
 1039 Open or solid dots indicate seasonal values (Pg C season⁻¹) and vertical bars indicate annual sum
 1040 (Pg C yr⁻¹). Data are shown for: (a) boreal and temperate Northern Hemisphere (BoTeNH, >
 1041 23.5°N), (b) tropics and extratropical Southern Hemisphere (TroSH, < 23.5°N) and (c) the whole
 1042 globe. Solid dots indicate seasonal land carbon uptake anomalies below 10th or above 90th
 1043 percentiles over 1981-2015.

1044



1045
 1046 **Figure 6** Extremeness of transitions in seasonal land carbon uptake anomaly in 2015. Lines of
 1047 histograms for seasonal land carbon uptake transitions over 1981-2015 are shown for boreal and
 1048 temperate Northern Hemisphere (BoTeNH, latitude > 23.5°N), tropics and extratropical Southern
 1049 Hemisphere (TroSH, latitude < 23.5°N) and the whole globe. Transition between two
 1050 consecutive seasons is defined as the linearly de-trended land carbon uptake anomaly in a given
 1051 season minus that in the former one. Horizontal-axis shows the seasonal transitions in land
 1052 carbon uptake anomalies (Pg C season⁻¹). Vertical orange solid lines indicate values for 2015.
 1053